Article

The rational design, synthesis and antimicrobial properties of thiophene derivatives that inhibit bacterial histidine kinases.

Thibaut Boibessot, Christopher P. Zschiedrich, Alexandre Lebeau, David Bénimèlis, Catherine Dunyach-Rémy, Jean-Philippe Lavigne, Hendrik Szurmant, Zohra Benfodda, and Patrick Meffre

J. Med. Chem., **Just Accepted Manuscript** • DOI: 10.1021/acs.jmedchem.6b00580 • Publication Date (Web): 30 Aug 2016

Title: The rational design, synthesis and antimicrobial properties of thiophene derivatives that inhibit bacterial histidine kinases

Authors: Thibaut Boibessot[†#],Christopher P. Zschiedrich[‡#], Alexandre Lebeau[†], David Bénimèlis[†], Catherine Dunyach-Rémy[§], Jean-Philippe Lavigne[§], Hendrik Szurmant*[‡Ψ], Zohra Benfodda*[†ϖΨ], Patrick Meffre[†ϖΨ]

[†] UNIV. NIMES, EA7352 CHROME, Rue du Dr G. Salan, 30021 Nîmes cedex 1, France.

[‡] Basic Medical Sciences, College of Osteopathic Medicine of the Pacific, Western University of Health Sciences, Pomona, CA 91766, USA and Department of Mol. & Exp. Medicine, The Scripps Research Institute, La Jolla, CA 92037, USA

[ϖ]IBMM, UMR-CNRS5247, Université de Montpellier, Place Eugène Bataillon, 34095 Montpellier, France.

[§]Institut National de la Santé et de la Recherche Médicale, U1047, Montpellier University, CHU de Nîmes, Place du Pr R. Debré, 30029 Nîmes.

Keywords: Two-component system, histidine kinase, thiophene derivatives, rational design, molecular docking, antibacterial agents, bacterial resistance

ABSTRACT

The emergence of multi-drug-resistant bacteria emphasizes the urgent need for novel antibacterial compounds targeting unique cellular processes. Two-component signal transduction systems (TCSs) are commonly used by bacteria to couple environmental stimuli to adaptive responses, are absent in mammals, and are embedded in various pathogenic pathways. To attenuate these signaling pathways, we aimed to target the TCS signal transducer histidine kinase (HK) by focusing on their highly conserved adenosine triphosphate (ATP)-binding domain. We used a structure-based drug design strategy that begins from an inhibitor-bound crystal structure and includes a significant number of structurally simplifiying "intuitive" modifications to arrive at the simple achiral, biaryl target structures. Thus, ligands were designed, leading to a series of thiophene derivatives. These compounds were synthesized and evaluated in vitro against bacterial HKs. We identified eight compounds with significant inhibitory activities against these proteins, two of which exhibited broad-spectrum antimicrobial activity. The compounds were also evaluated as adjuvants for the treatment of resistant bacteria. One compound was found to restore the sensivity of these bacteria to the respective antibiotics.

1. INTRODUCTION

Antibiotics are considered among the most important medical discoveries of the 20th century. Unfortunately, the clinical use of conventionally available antibiotics has led to the rapid development of resistance .[1–3] One of the first clinical antibiotics, penicillin, was introduced in the mid-1940s and resistant mutants appeared within 2 years of its introduction.[4] After 75 years of extensive antimicrobial use against strains of *Salmonella enterica*, a leading cause of bacterial gastroenteritis, several bacteria have become resistant to front line antibiotics, and the emergence of *methicillin-resistant Staphylococcus aureus* (MRSA) strains has increased in nosocomial and community settings.[5–7] The high level of inherent antibiotic resistance in *Pseudomonas aeruginosa* makes the treatment of cystic fibrosis problematic.[8] In contrast, the pharmaceutical companies' investments in the discovery and development of new antibiotics have stagnated compared with their investments in drugs combatting chronic diseases such as cancer and diabetes.[9] Antimicrobial resistances is not only a major health problem but is also an economic issue.[10] Hence, innovative research to develop anti-infective agents with novel modes of action that circumvent the current resistance mechanisms is urgently needed. [11–13]

Bacteria have evolved a variety of mechanisms to respond to environmental changes. Among the most commonly utilized are two-component signal transduction systems (TCSs). [14] TCSs were proposed as attractive targets because they are absent in mammals and essential or conditionally essential for viability in several important bacterial pathogens.[15–23] To respond to diverse environmental changes, a bacterium typically possesses multiple TCSs.[24–26] These TCSs are implicated in survival roles and pathogenic mechanisms, such as nutrient acquisition, sporulation, biofilm formation and antibiotic resistance.[27,28] TCS inhibitors are expected not only to work as antibacterial agents but also to be developed as adjuvants with known antimicrobials to target drug resistance, colonization or virulence factor expression.[22,29,30] Most commonly, a TCS consists of a membrane-spanning sensor HK and a cytosolic

transcription factor, termed the response regulator (RR); however many variations including soluble HK and non-transcription factor RR proteins, exist. In response to an environmental or cellular signal, HKs autophosphorylate a conserved histidine residue in the dimerization domain and the phosphoryl group is subsequently transferred to a conserved aspartic acid in the regulatory domain of its paired RR. The phosphorylated RR typically binds to the promoter regions of target genes modulating their expression (Figure 1).[31] Interest in deactivating TCS transduction by targeting the catalytic and adenosine triphosphate (ATP)-binding (CA) domain of the HK has increased.[32,33] The catalytic core within HKs has been reported to exhibit a high degree of homology in both Gram-positive and Gram-negative bacteria.[34,35] This degree of homology suggests that a single agent targeting this CA domain could inhibit multiple TCSs simultaneously. Consequently, bacterial resistance would be less likely to develop.

The search for inhibitors capable of interrupting TCS has yielded several classes of effective HK inhibitors.[30] Unfortunately many of them suffer from poor bioavailability stemming from their highly hydrophobic properties.[21,22,36] Some other inhibitors have demonstrated poor selectivity and appear to cause protein aggregation.[32]Finally, some inhibitors lead to hemolysis.[37] More recently, several interesting reports have described the experimental or *in silico* identification of specific inhibitors against the essential cell wall homeostasis regulator kinase WalK with antimicrobial activity against some Gram-positive organisms.[38,39] However, currently whether these compounds are of clinical value and whether the focus on a single kinase might greatly reduce the spectrum of these compounds are unclear. An approach to identify broad spectrum inhibitors of HK proteins has been published while this manuscript was in preparation employing a combination of fragment based screening and in silico docking technology.[40] Also of note, HK activation rather than inhibition has also recently been described as a strategy to control virulence of Gram-negative bacteria, since avirulent

Salmonella and *Haemophilus* species commonly have mutations that lead to constitutive activation of the conjugative plasmid expression TCS CpxRA. [41] The development of new inhibitors capable of disrupting TCS signaling remains a challenging. In the present study, we used a structure-based drug design strategy, based on the crystal structure of the ATP pocket of essential cell wall homeostasis regulator kinase WalK (Protein Data Bank [PDB]: 3SL2), and PLANTS as a virtual screening software to identify new inhibitors of HK. To this end, we utilized the fact that HKs share a related CA domain with DNA-gyrases and topoisomerases. The latter represent known antimicrobials targets, and high-resolution structures of inhibitor-bound proteins exist. HK ligands were designed leading to the development of a series of thiophene derivatives (**6a-6u**, **7a-7c, 8a-i**). These compounds were synthesized, and their inhibitory properties were evaluated against three bacterial HK proteins, *B. subtilis* phosphate limitation sensor kinase PhoR, respiration sensor kinase ResE, and kinase WalK. Their antimicrobial activities against nine bacterial strains were assessed. Moreover, the compounds were evaluated as adjuvants against antibiotic-resistance bacterial strains. We identified several compounds with desirable activities against HKs. These lead compounds represent potential starting points for future HK inhibitor development.

2. RESULTS AND DISCUSSIONS

2.1 Design of new compounds.

To generate HK inhibitors, we utilized a structure-based design methodology. Inhibitors are expected to exhibit antibacterial properties when a single essential TCS is targeted or when multiple systems whose activities function not necessarily alone but in combination are targeted simultaneously. Our aim was to inhibit multiple HKs simultaneously and to make evolving resistance more difficult. We decided to target the ATP-binding domain because this strategy was very recently validated[29,42]. The ATP-binding domain is characterized by a Bergerat fold, which is a domain shared with DNA-gyrases and topoisomerase, heat shock

proteins and the mutator protein MutL protein. The Bergerat fold consists of a sandwich of α-helices in one layer, and mixed β-strands in another, and a discrete and flexible ATP lid[43–45]. To design the inhibitors, we used the available X-ray structure of the ATP-binding domain of WalK (PDB: 3SL2[46]) at a resolution of 1.61 Å. This structure comprises a two-layer α/β sandwich-fold with a large ATP pocket (Figure 2A). One layer is composed of a five-stranded β-sheet. Strands 1 and 2 run parallel, whereas the directions of strands 2, 3, 5 and 4 alternate. The second layer is made of three α-helices. These two layers are linked by a large flexible loop (Asp533–Gly567) containing a short helical segment that is crucially involved in ATP binding[46]. This loop is designated as the ATP-lid. The interactions among ATP, Asp533 and Water822 are known to be critical for protein-cofactor binding. Additionally, we observed π-stacking between the adenine ring and Tyr507 (Figure 2B). Thus, our aim was to design ligands that can form hydrogen bonds and hydrophobic interactions with these elements.

As mentioned above, the ATP-binding domain of the TCS, a Bergerat fold, is also found in Gyrase B, heat shock protein Hsp90, histidine kinases and mutator protein MutL[44,47]. The PDB was probed for structures of ligand-bound domains of these proteins to investigate inhibitor binding modes. Gyrase B was singled out because several Gyrase B-ligand complexes are available with affinities in the nanomolar range.[48–50] Moreover, a Gyrase B ligand has been reported to bind to the ATP-domain of HKs.[45,47] We decided to focus on the complex PDB: 3TTZ because the ligand 2-[(3S,4R)-4-{[(3,4-dichloro-5-methyl-1H-pyrrol-2-yl)carbonyl]amino}-3-fluoropiperidin- 1-yl]-1,3-thiazole-5-carboxylic acid (pyrrolamide, Figure 3 D) has an 50% inhibitory concentration (IC_{50}) value of 4 nM.[49] Comparative docking was performed according to the typical protein kinase protocol.[51,52] Known ligands were transferred from the template structure into the target structure. The deduced protein–ligand complexes were visualized and the protein–ligand interactions were evaluated. To transfer the ligand of Gyrase B into the HK CA domain, we first superimposed the two structures with a

root mean square deviation (RMSD) of 0.740 Å using ViTO (Figure 3A).[53] The Gyrase B pyrrolamide ligand (Figure 3D) was then transferred into histidine kinase CA domain and evaluated with DSX (Figure 3B and 3C).[54] We observed that the ligand forms a hydrogen bond with Asp533 in the bottom of the pocket; however, significant steric hindrance exists at the edge of the pocket with Ile536 and Tyr507. Furthermore, the electronic effects in the edge of the pocket are dissimilar in Gyrase B and HK WalK. Indeed, in Gyrase B, the edge of the pocket appear to be charged. Arg84 and Glu58 form a salt bridge, and Arg144 interacts with the acidic moeity of the pyrrolamide inhibitor. In contrast, in the HK WalK, the edge of the pocket appears to be relatively hydrophobic as noted in the presence of Tyr507, Leu568 and Ile536.

These observations guided our strategy for designing the HK ATP-binding domain inhibitors of type **6**. Our thought process is visualized in Figure 4. We noted that after scoring the pyrrolamide ligand the -NH of the pyrrole moiety forms a hydrogen bond with Asp533, and the C=O of the amide bond establishes a hydrogen bond with Water822. Consequently, we rigidified the amide bond viaa cyclization to produce structure A in Figure 4. We added an aromatic ring to maintain hydrophobicity because the edge of the pocket in the HK WalK (and others) is hydrophobic and because doing to imbues pyrrolamide with a plane-like geometry, generating structure B (Figure 4). As mentioned above, steric hindrance occurs at the edge of the pocket, and thus, the size of requiring size ligand must be reduced.Therefore, we removed the piperidine ring and the chirality, which is often difficult to control in chemical synthesis, which produced a subtituted phenyl ring (Figure 4, structure C). Finally, we chose a thiophene ring instead of a thiazole to gain easy and quick access to a series of compounds of type 6 as shown in Figure 4.

Initially, a virtually focused chemical library was designed based on general structure **6** (Figure 5) to form hydrogen bonds with Asp533 and hydrophobic interactions with Tyr507.

This library was constructed to be easily accessible chemically. Thus, in positions R1, R2 and R3, we preferred to derivatize the phenyl ring with only one substituent, which can be either a hydrogen bond donor or acceptor. In position R', we chose to add polar substituents to increase the compounds' solubility. We docked this virtual chemical library into the ATP-binding site of WalK (PDB: 3SL2) using PLANTS[55]. Protein and ligands were prepared with SPORES[56,57] before docking and the docking poses were reevaluated using the DSX[54] scoring function. When inspecting the docking poses, the phenyl ring can be observed at the bottom of the pocket, and the substituent points in the direction of Asp533. The thiophene ring participates in π-staking with Tyr507, and the polar substituents note of the pocket towards the solvent (Figure 6A and 6B). When comparing the binding poses and the scores obtained from both the docking and reevaluation experiments (Table 1), 21 compounds in the virtual library were considered promising and singled out for synthesis.

2.2 Synthesis

Thiophene derivatives (**6a-u**) were synthesized using the palladium-catalyzed Suzuki-Miyaura cross-coupling reaction (Scheme 1).[58] Various commercially available phenyl boronic acid derivatives (**5a-5g**) were reacted with commercially available 2-bromo-5-nitrothiophene (**1**), 2-acetyl-5-bromothiophene (**2**), and easily generated 2-acetamide-5-bromothiophene (**3**). **3** was prepared according to the literature.[59] Indeed, the reaction between 2-acetyl-5-bromothiophene (**2**) and hydroxylamine hydrochloride gave a mixture of two isomeric oximes (**4a-b**), which were separated by column chromatography, yielding the respective isomers E **4a** (54%) and Z **4b** (45%) (Scheme 2). Then, isomer E (**4a**) was used in a Beckmann rearrangement to give the acetamide **3** in 88% yield.

For the Suzuki reaction (Scheme 1), $Pd(PPh_3)_4$ or $PdCl_2(PPh_3)_2$ was used as the catalyst; Na_2CO_3, or K_2CO_3 or Cs_2CO_3 was used as the base; and typical solvents were used (for more details see the Supporting Information). The reactions were conducted at 70°C-90°C, and

moderate to good yields of the desired compounds (**6a-u**) were obtained (Table 2). The Suzuki coupling gave complete conversion in all cases, although the work up and purification were cumbersome. Compounds **6a-c** reacted with 2-iodoethanol at 90°C under inert conditions in N,N-dimethylformamide (DMF) or without a solvent to produce compounds (**7a-c**) in moderate yields (Scheme 3, Table 2).

To overcome the solubility problems encountered during biological evaluations, we decided to synthesize the hydrochloride salts of the amines. Treating the amines (**6a-c, g-i, and m-o**) with 12-N HCl in tetrahydrofuran (THF) or with *in situ*-generated HCl afforded the amines as their HCl salts **8a-i** in moderate to good yields (Scheme 4).

The final compounds **6a-u**, **7a-c,** and **8a-i** were fully characterized by ^{1}H nuclear magnetic resonance (NMR), ^{13}C NMR, infrared (IR) spectroscopy, high-performance liquid chromatography (HPLC) and high-resolution mass spectrometry (HRMS). The mass spectra displayed the correct molecular ions peaks because the measured HRMS data are in good agreement with the calculated values (see theSupporting Information).

The designed compounds **6a-u** and **7a-c** were then evaluated against different HK proteins.

2.3 Biological evaluation of compounds

2.3.1 Several compounds exhibit inhibitory activity against the HK WalK

In an initial screening, compounds **6a-u** and **7a-c** were evaluated for their ability to inhibit the autophosphorylation activity of HK WalK from *Bacillus subtilis.* To this end, two distinct cytoplasmic WalK constructs were utilized, WalK$^{204-612}$ and WalK$^{272-612}$. Both constructs share a catalytic core, including the ATP-binding Bergerat fold or CA domain of the kinase, but the longer construct contains an additional N-terminal HAMP domain. We argued that both fragments should behave similarly with regard to potential compound inhibition suggesting that these compounds indeed target the catalytic portion of the proteins. When screening with equimolar concentrations of the compounds and ATP, eight (**6c**, **6d**, **6e, 6h**, **6i**,

6k, **6s**, and **7c**) of the 24 compounds were observed to significantly inhibit the kinase activity (Figure 7). Six of the eight compounds inhibited both fragments of the kinase to similar extents, whereas two compounds, **6h** and **6i**, inhibit the longer WalK fragment to a greater extent than the shorter one. Regardless, these eight compounds were considered as potentially interesting HK inhibitors and were subjected to more-detailed downstream evaluations.

2.3.2 Some compounds inhibit multiple HKs

A desirable trait for any HK inhibitor is to be capability to specifically inhibit multiple HKs of in organism, rather than a single HK, because it is more difficult for a bacterium to acquire resistance against a multi-target inhibitor as such inhibitors could be expected to have a broader antimicrobial spectrum. To assess whether the eight compounds that inhibited WalK *in vitro* also inhibited other HKs, we utilized *B. subtilis* HKs PhoR, which is involved in the detection of phospholimitation, and HK ResE, which is involved in the transition to anaerobic conditions. The IC_{50} values were determined against all three HKs. Because the kinase serves as both, the substrate and enzyme in this assay, the concentration of the enzyme is higher than those of most other proteins, and as a result, the lower limit for the IC_{50} values is in the low μM range rather than in the nM range. A typical assay for compound **6e** is depicted in Figure 8A, demonstrating that this compound inhibits all three HKs to varying extents. Similar results were obtained for the other seven compounds and the IC_{50} values are summarized in Table 4. Screens were also performed with the *B. subtilis* sporulation HK KinA, resulting in similar inhibition patterns: the IC_{50} values were not determined for this kinase (data not shown). Of note, one compound **6s** showed significantly better inhibition of PhoR (IC_{50}: 1.6 μM) than ResE and WalK, demonstrating that selectivity can be achieved by varying phenyl group substituents. At this point we can only speculate why this compound would be selectively inhibiting PhoR. The docking pose in Figure 6 suggests that the phenyl group substituents are in contact with conserved Asp533 deep within the ATP binding pocket. This

pocket might be more accommodating for increased size of substituents in PhoR or might make additional contacts with these substituents. In summary, the eight compounds could inhibit the autophosphorylation activity of multiple different HKs in vitro.

2.3.3 The compounds do not inhibit the serine/threonine kinase IreK

Based on the results thus far, the eight compounds possibly inhibited enzymatic activity non-specifically or inhibited protein kinases in general rather than only HKs. This trait would be an undesirable because kinases are abundant and essential proteins in all domains of life. To ensure that the eight compounds did not inhibit kinases with different structures and activities, we utilized the structurally unrelated eukaryotic-like serine/threonine kinase IreK (intrinsic resistence of enterococci kinase) of *E. faecalis*, which also utilizes ATP as a phosphoryl-group donor. The IC_{50} values were determined for concentrations of up to 800 μM of each compound, analogous to the HK inhibition assays. A typical assay is shown for compound **6e** is shown in Figure 8B. The results for all compounds were identical and are summarized in Table 4. We observed no inhibition of the serine/threonine kinase IreK, suggesting that the eight compounds target HKs specifically and do not merely inhibit any enzyme or any kinase.

2.3.4 The compounds do not significantly inhibit E. coli DNA-gyrase

ATP-dependent DNA-gyrases and topoisomerases catalyze essential bacterial DNA-packing processes and utilize an ATP-binding domain that is structurally related to that in HKs. This fact was utilized to design the current compound series starting with a known gyrase inhibitor. Thus, the novel compounds possibly not only inhibited HKs but also targeted DNA-gyrase. To investigate whether the eight compounds with activity against HKs also inhibited DNA-gyrase activity, we utilized the commercially available *E. coli* DNA-gyrase. To this end, a standard gyrase assay was utilized, where relaxed plasmid DNA was exposed to DNA-gyrase in the absence or presence of varying amounts of the eight compounds. As a control, we utilized a known gyrase inhibitor and antibiotic, ciprofloxacin at a concentration of 200 μM.

Whereas ciprofloxacin completely inhibited the ability of DNA-gyrase to induce the supercoiling of relaxed plasmid DNA, the eight compounds showed no or little inhibitory activity up to a concentrations of 800 μM. A typical assay of compound **6e** is shown in Figure 8C. The IC_{50} values for all eight compounds are summarized in Table 4. Although all compounds exhibited IC_{50} values for DNA-gyrase that were much larger than those observed for the HKs, some compounds-**6c**, **6d**, **6k** and **7c-** inhibited DNA-gyrase at the highest tested concentrations. In summary, the eight compounds show a preference for HKs but we cannot conclude that the gyrases and topoisomerases from some organisms will not also be subject to inhibition by some of these compounds.

2.3.5 The compounds **6d** and **6e** exhibit significant antimicrobial activity

Given these promising *in vitro* HK inhibition data, we wondered whether any of these tested compounds exhibited antimicrobial activity. To this end, we screened the eight compounds against HK activity in a standard Kirby-Bauer disk diffusion assay against MRSA TCH1516 USA300. Paper disks containing 100 μg of each of the eight respective compounds were placed on plates with growing lawns of *Staphylococcus aureus*. Following incubation clear rings of growth inhibition could be observed for two of the eight compounds **-6d** and **6e-** analogous to a vancomycin control; no growth inhibition was observed for the other six compounds (Figure 9A). To further investigate whether this growth inhibition was significant a similar assay was perfomed with decreasing concentrations of compounds **6d** and **6e** (Figure 9B). The diameter of the ring of growth inhibition did not change even when only 20 μg of compound was used per disk. A reduced ring of growth inhibition was identified using 4 μg of compound **6e**.

These promising results prompted us to quantify the antimicrobial activity of compounds **6d** and **6e** against nine selected bacteria including several important human pathogens. To this end, we utilized the Clinical & Laboratory Standards Institute (CLSI) two-fold serial broth-

dilution method to determine the minimum inhibitory concentration (MIC), which is defined as the concentration at which no bacterial growth can be observed, and the minimum bactericidal concentration (MBC), which is defined as the concentration at which 99.99% of bacteria are killed. The data from these assays are summarized in Table 5. Clearly both, compounds **6d** and **6e** exhibit activity against Gram-positive and Gram-negative bacteria. *E. faecalis* appeared to be the least susceptible of the tested bacterial strains. In general, both compounds showed very similar inhibition spectra, but compound **6d** seemed to be slightly more potent than **6e**.

In summary, of the eight identified HK inhibitors, two exhibited broad-spectrum antimicrobial activity against different significant pathogens.

2.3.6 The compounds **6d** and **6e** are bactericidal rather than bacteriostatic

Antimicrobials are usually classified as either bacteriostatic or bactericidal. Whereas the former merely inhibit growth, the latter induce the lysis and killing of cells. It is typically thought that bacteriostatic antimicrobials inhibit cellular processes such as transcription or translation, whereas bactericidal antibiotics target the cell envelope. To test whether compounds **6d** and **6e** were bacteriostatic or bactericidal, we grew cultures of *B. subtilis* (Fig. 9C) and MRSA (not shown) in the absence or presence of 50 μg/ml compounds **6d** or **6e**. As a control bacteriostatic antibiotic, we utilized chloramphenicol and as a control bactericidal compound we utilized vancomycin. We observed that compound **6d** behaved very similarly to vancomycin in this assay, inducing slow bacterial lysis over a time course of 9 h. In contrast, compound **6e** induced more rapid cell lysis and clearing of the culture than either vancomycin or compound **6d** (Fig. 9C). In summary, compounds **6d** and **6e** appear to be bactericidal rather than bacteriostatic.

2.3.7 The compounds do not exhibit hemolytic activity against sheep red blood cells

Several previously identified HK inhibitors were demonstrated to not be useful because they exhibited significant hemolytic activity. Thus, the bactericidal effects of compounds **6d** and **6e** possibly were attributable to unspecific lytic activity. To ensure that the compounds of interest, primarily compounds **6d** and **6e,** but also the other HK inhibitors, did not exhibit hemolytic activity, we utilized sheep red blood cells and a standard hemolysis protocol (material and methods). When sheep red blood cells were exposed to large concentrations (up to 1 mM) of the compounds, no hemolysis was observed (not shown), demonstrating that none of the compounds were hemolytic. This finding suggests that the antimicrobial activities of compounds **6d** and **6e** are not merely attributable to the unspecific induction of cell lysis.

2.3.8 The relatively soluble HCl salts of amines do not improve antimicrobial activities or HK inhibition

Several of the eight tested compounds showed very low solubility, which we suspected may have contributed to the lack of antimicrobial activity among some of them. To test whether increasing solubility of any of these compounds would positively affect their antimicrobial activities, we evaluated the HCl salts of the amines of compounds **6c**, **6h** and **6i**. These compounds did indeed show higher solubility in aqueous solutions. However, antimicrobial activity was not observed for any of the HCl salts according to the Kirby Bauer disk diffusion method (data not shown). Exposing PhoR kinase to these compounds also revealed that the HCl salts were significantly less-potent HK inhibitors than their less-soluble counterparts (data not shown). This finding is consistent with the idea that the amino groups of compounds **6c**, **6h** and **6i** contribute significantly to their interactions with and inhibition of kinases. Indeed, according to the design and docking studies, the amino group is expected to create a hydrogen bond with the conserved Asp533 residue in the HK, which is usually involved in binding of ATP (Figure 6). In summary, the HCl modification of this group is not a useful

strategy to improve the potency of the HK inhibitors, and thus, other strategies to increase solubility should be explored.

2.3.9 Adjuvant activity

Because TCSs are involved in increasing the fitness and adaptability of bacteria, we wondered whether sublethal concentrations of some of the compounds might exhibit adjuvant activity, rendering various antimicrobial resistant strains sensitive to the relevant antibiotic. All compounds were evaluated in association with several antibiotics, and one compound showed clear evidence of adjuvant activity. Table 6 shows the results obtained for compound **6d**. The use of **6d** in association with several antibiotics restored the sensitivity of the resistant isolates tested. Indeed, **6d** exerted this effect in both species evaluated (*E. coli and S. aureus*), regardless of the resistance mechanism involved. For example, for the extended spectrum beta lactamase (ESBL) *E. coli* isolate (ARS 108), the MIC values were >8 μg/mL when cefotaxime was used alone and <0.03 μg/mL after the addition of **6d** as an adjuvant. For *S. aureus*, identical results were found for the C1P15 penicillin G-resistant isolate and the C1BP13 MRSA isolate. However, the addition of **6d** did not restore the bactericidal effect of ofloxacin in the G02-resistant strain. These results show that TCS inhibitor **6d** presented potent bactericidal activity when used alone at concentrations over 32 μg/mL or as adjuvant combined with an antibiotic at the sublethal concentration of 25 μg/mL for all isolates and tested antibiotics.

In the current context, with the emergence of multi-resistant bacteria, such as MRSA and ESBL *E. coli*, becoming a serious public health problem in terms of therapeutic management, these results showing that one HK inhibitor (**6d**) could able to restore the sensitivity of resistant isolates, regardless of the mechanism involved, are encouraging.[60,61] This effect may be attributable to the inhibition of HK, which could prevent the expression of the genes responsible for the development of resistance mechanisms.

3. CONCLUSIONS

In this study, we designed and synthesized a series of thiophene derivatives as potential HK inhibitors. Eight of the compounds target HK WalK and inhibit the autophosphorylation activity of this essential HK. Among these eight compounds, all were able to inhibit multiple HKs, and the IC_{50} values were determined. Moreover, they do not inhibit the serine/threonine kinase IreK or *E. coli* DNA-gyrase. Two of the compounds exhibit significant antimicrobial activity, and none of the eight compounds have hemolytic activity against sheep red blood cells. Finally, the use of one of the HK inhibitors (**6d**) as an adjuvant in association with the antibiotics tested (amoxicillin or cefotaxim) restored the sensitivity of drug-resistant isolates. As the number of multidrug resistant bacteria, such as MRSA and ESBL *E. coli*, increases, the need to develop different strategies to fight these infections is becoming more urgent. The compounds identified here can be considered as initial leads for the development of improved antibacterial agents.

4. EXPERIMENTAL SECTION

4.1. Computational Studies: Preparation of Enzyme and Compounds for Docking

The crystal structure of the ATP-binding domain of Histidine kinase WalK was extracted from Protein Data Bank (PDB code: 3SL2).[46] All the water molecules except water822 and heteroatoms were removed. The protein was completed, hydrogen atoms were added, and reprotonated with SPORES.[57] The chemical structures of all the synthesized compounds were generated using Marvin sketch and were subsequently converted into 3D format using Open Babel[62] and prepared with SPORES. A serie of docking experiment were carried out with all the designed compounds against the ATP-binding domain of WalK using PLANTS for possible Histidine kinase inhibition activities. The compounds were selected on the basis of their scores and their pose, all compounds were re-scored with DSX.[54] As a parameter for the molecular docking, the ant algorithm was set to 1 (highest reliability). The pocket is a 30Å radius center on Asp533 making sure those inhibitors can fit in the active site. The number of poses was set to 10 with a clustering RMSD of 2Å and the pyrrole and amide bond of the pyrrolamide inhibitor was used as a shape constraint. Tyr507, Ile536 and Asn503 were set as flexible side chains. The PLANT scoring function was set to chemplp and sulfur acceptors were enabled. The finally obtained docked complexes were subsequently visualized using PyMol.

4.2. Chemistry.

General. All reagents were purchased from the Aldrich Chemical Co. and used without any purification. Solvents were distilled from the appropriate drying agents immediately prior to use. NMR spectra were recorded with a Bruker Avance 300 spectrometer (300 and 75 MHz for ^{1}H and ^{13}C NMR, respectively). Chemical shifts (δ) and coupling constants (*J*) are given in ppm and Hz, respectively, using residual solvent signals as reference for the ^{1}H and ^{13}C. The following abbreviations are used: s = singlet, d = doublet, t = triplet, q = quartet, br s = broad

signal, dd = double doublet, dt = double of triplet, m = multiplet. High resolution mass spectra (HRMS) were obtained by electrospray using a TOF analyzer Platform. IR spectra were obtained using a Jasco FT-IR 410 instrument as a thin film on NaCl disc as stated; only structurally important peaks ($\bar{\upsilon}$) are presented in cm^{-1}. Reactions were monitored with Merck Kieselgel $60F_{254}$ precoated aluminium silica gel plates (0.25 mm thickness). Melting points were determined on a Stuart scientific SMP10 apparatus and are uncorrected. Flash chromatography were performed on a Grace Reveleris X2 using 40µm packed silica cartridge. Flash chromatography experiments were carried out on Silica Gel premium Rf grade (40-63 µm) or were performed on a Grace Reveleris X2 using 40µm packed silica cartridge. HPLC analyses were obtained on the Waters Alliance 2795 using the following conditions: thermo Hypersil C18 column (3 µm, 50 mm L x 2.1 mm ID), 20°C column temperature, 0.2 mL/min flow rate, photodiodearray detection (210-400 nm), mobile phase consistent of a gradient of water and acetonitrile (each containing 0.1% trifluoroacetic acid). UPLC analyses were obtained on the Waters Acquity H-Class using the following conditions: Waters Acquity BEH C18 column (1.7µm, 50 mm x 2.1 mm), 25°C column temperature, 0.5 mL/min flow rate, photodiodearray detection (TUV – 214nm), mobile phase consistent of a gradient of water and acetonitrile (each containing 0.1% of formic acid). The purity of all synthetic compounds was determined by HPLC analysis and was greater than 95%.

(E) and (Z)-2-(5-bromo-2-thienyl)prop-1-en-1-ol (**4a** and **4b**). Compounds **4a** and **4b** were prepared according to a procedure described by Lucas or minor modifications thereof.[59] A solution of 2-acetyl-5-bromothiophene (**2**) (4.0 g, 19.5 mmol), hydroxylamine hydrochloride (1.63 g, 23.4 mmol) and sodium acetate trihydrate (3.18 g, 23.4 mmol) in a mixture of absolute ethanol and water (55 mL, 4/1, v/v) was heated under refluxed for 3 hours. The solvent was removed in vacuo and the residue was purified by column chromatography (40-63 µm) on silica using a mixture of CH_2Cl_2/MeOH (98/2, v/v) to give the oxime **4a** (2.33 g,

54%) as white solid; mp 134-136 °C; R_f 0.35 (CH_2Cl_2). ^{1}H NMR (DMSO-d_6) δ: 2.12 (s, 3H, CH_3), 7.16 (d, 1H, J = 4.0 Hz), 7.18 (d, 1H, J = 4.0 Hz), 11.34 (s, 1H, N-OH). ^{13}C NMR (DMSO-d_6) δ: 11.2 (CH_3), 112.4 (C), 126.9 (CH), 130.6 (CH), 142.6 (C), 149.3 (C). IR: 3233 ($\bar{\upsilon}_{OH}$), 1428 ($\bar{\upsilon}_{C=N}$), 781 ($\bar{\upsilon}_{C-Br}$). Moreover, using a mixture of CH_2Cl_2/MeOH (80/20, v/v) to give the oxime **4b** (1.90 g, 45%) as a white solid; mp 175-177 °C; R_f 0.06 (CH_2Cl_2). ^{1}H NMR (DMSO-d_6) δ: 2.23 (s, 3H, CH_3), 7.27 (d, 1H, J = 4.1 Hz), 7.31 (d, 1H, J = 4.1 Hz), 11.89 (s, 1H, N-OH). ^{13}C NMR (DMSO-d_6) δ: 18.4 (CH_3), 117.4 (C), 128.6 (CH), 129.1 (CH), 133.1 (C), 144.9 (C). IR: 1411 ($\bar{\upsilon}_{C=N}$), 791 ($\bar{\upsilon}_{C-Br}$) (The IR spectra show no absorption band for the –OH stretching in according to the litterature).[63]

N-(5-bromo-2-thienyl)acetamide (3). Compounds **3** was prepared according to a procedure described by Lucas or minor modifications thereof.[59] To a solution of **4a** (2.330 g, 10.6 mmol) in a mixture of acetone and water (54 mL, 3.5/1, v/v) was added 4-methylbenzene-1-sulfonyl chloride (2.231 g, 11.7 mmol) and sodium hydroxide (0.468 g, 11.7 mmol) at 0°C. The reaction was allowed to warm to room temperature and heated to 60 °C during 1.5 hours. After cooling to room temperature, the solvent was removed in vacuo. The residue is dissolved in ethyl acetate (150 mL) and washed with water (3*40 mL), aqueous saturated $NaHCO_3$ (3*40 mL) and brine (3*40 mL). The organic layer was dried over $MgSO_4$, filtered and concentrated. The residue was purified by flash chromatography (silica gel, PE/EtOAc; 10/90 ramping to 100/0) provided **3** (2.054 g, 88%) as a pale grey solid; mp 135-137 °C; R_f 0.20 (PE/EtOAc: 40/60; v/v). ^{1}H NMR (DMSO-d_6) δ: 2.06 (s, 3H, CH_3), 6.41 (d, 1H, J = 4.1 Hz), 6.94 (d, 1H, J = 4.1 Hz), 11.40 (s, 1H, NH). ^{13}C NMR (DMSO-d_6) δ: 22.2 (CH_3), 102.4 (C), 109.8 (CH), 126.6 (CH), 140.4 (C), 166.7 (CO). IR: 3242, 3202 ($\bar{\upsilon}_{NH}$), 1562 ($\bar{\upsilon}_{C=O}$), 781 ($\bar{\upsilon}_{C-Br}$).

General Synthetic Procedure A for the synthesis of **6a-6c** and **6g-6i**. Compounds **6a-6c** and **6g-6i** were prepared according to a procedure described by Slevin et al. or minor

modifications thereof.[64] To a solution of the thiophene (2.30 mmol), the corresponding aminophenylboronic acid (HCl salt) (2.30 mmol) and $Pd(PPh_3)_4$ (5 mol%) in a mixture of toluene/ethanol (16 mL, 2.3/1, v/v) was added 2M aqueous sodium carbonate (4.5 mL). The mixture was refluxed during 16 hours. The cold solution was diluted with ethyl acetate (50 mL), filtered through a Celite pad and the filtrate was diluted with water (60 mL). The aqueous solution was extracted with ethyl acetate (3*50 mL). The organic phases were combined, dried over $MgSO_4$, filtered, and concentrated under reduced pressure to give the crude compound. The residue was purified by flash column chromatography (silica gel, AtOAc/PE, 0/100 ramping to 100/0, v/v) to give the desired compound.

*2-(5-nitro-2-thienyl)benzenamine (**6a**).* The desired product was dissolved in a small amount of ethyl acetate and 150 mL of cold pentane (-20°C) was added, resulting in precipitation of a solid. The solid was filtered, washed twice with 20 mL of cold pentane and suction-dried to yield **6a** as a red solid; R_f 0.30 (PE/EtOAc: 80/20; v/v). ^{1}H NMR (DMSO-d_6) δ: 5.47 (s, 2H, NH_2), 6.68 (t, 1H, J = 7.5Hz), 6.86 (d, 1H, J = 8.1Hz), 7.16 (t, 1H, J = 7.7Hz), 7.33 (d, 1H, J = 7.7Hz), 7.42 (d, 1H, J = 4.4Hz), 8.15 (d, 1H, J = 4.4Hz). ^{13}C NMR (DMSO-d_6) δ: 116.5 (C-NH_2), 117.1 (CH), 117.4 (CH), 125.7 (CH), 130.0 (CH), 130.8 (CH), 130.9 (CH), 146.4 (C), 148.5 (C), 150.7 (C). IR: 3434, 3356 ($\bar{\upsilon}_{NH2}$). HRMS: $[M + H]^+$ calcd for $C_{10}H_9N_2O_2S$, 221.0385; found, 221.0384.

*3-(5-nitro-2-thienyl)benzenamine (**6b**).* The desired product was dissolved in a small amount of ethyl acetate and 150 mL of cold pentane (-20°C) was added, resulting in precipitation of a solid. The solid was filtered, washed twice with 20 mL of cold pentane, and suction-dried to yield **6b** as an orange solid; R_f 0.24 (PE/EtOAc: 70/30; v/v). ^{1}H NMR (DMSO-d_6) δ: 5.40 (s, 2H, NH_2), 6.65-6.69 (m, 1H), 6.93-6.96 (m, 2H), 7.11-7.16 (m, 1H), 7.49 (d, 1H, J = 4.4Hz), 8.12 (d, 1H, J = 4.4Hz). ^{13}C NMR (DMSO-d_6) δ: 110.8 (CH), 113.7 (CH), 116.0 (CH), 123.2 (CH), 130.1 (CH), 131.4 (CH), 132.0 (C-NH_2), 148.6 (C), 149.6 (C),

152.9 (C). IR: 3439, 3342 ($\bar{\upsilon}_{NH2}$). HRMS: $[M + H]^+$ calcd for $C_{10}H_9N_2O_2S$, 221.0385; found, 221.0384.

*4-(5-nitro-2-thienyl)benzenamine (**6c**).* The desired product was dissolved in a small amount of ethyl acetate and 150 mL of cold pentane (-20°C) was added, resulting in precipitation of a solid. The solid was filtered, washed twice with 20 mL of cold pentane, and suction-dried to yield **6c** as a red solid; R_f 0.20 (PE/EtOAc: 70/30; v/v). ^{1}H NMR (DMSO-d_6) δ: 5.92 (s, 2H, NH_2), 6.62 (d, 2H, J = 8.6Hz), 7.36 (d, 1H, J = 4.5Hz), 7.52 (d, 2H, J = 8.6Hz), 8.06 (d, 1H, J = 4.5Hz). ^{13}C NMR (DMSO-d_6) δ: 113.9 (2CH), 118.5 (C-NH_2), 120.3 (CH), 127.8 (2CH), 132.1 (CH), 145.8 (C), 151.6 (C), 154.9 (C). IR: 3464, 3371 ($\bar{\upsilon}_{NH2}$). HRMS: $[M + H]^+$ calcd for $C_{10}H_9N_2O_2S$, 221.0385; found, 221.0386.

*1-(5-(2-aminophenyl)thiophen-2-yl)ethanone (**6g**).* Compound **6g** was obtained as a yellow powder; R_f 0.41 (PE/EtOAc: 60/40; v/v). ^{1}H NMR (DMSO-d_6) δ: 2.54 (s, 3H, CH_3), 5.27 (s, 2H, NH_2), 6.64 (td, 1H, J_1 = 7.7Hz, J_2 = 1.1Hz), 6.82 (dd, 1H, J_1 = 8.1Hz, J_2 = 0.9Hz), 7.08-7.13 (m, 1H, H_{AR}), 7.23 (dd, 1H, J_1 = 7.7Hz, J_2 = 1.4Hz), 7.38 (d, 1H, J = 3.9Hz), 7.93 (d, 1H, J = 3.9Hz). ^{13}C NMR (DMSO-d_6) δ: 26.4 (CH_3), 116.3 (CH), 116.9 (CH), 117.3 (C-NH_2), 126.6 (CH), 129.8 (CH), 130.0 (CH), 134.7 (CH), 142.0 (C), 145.7 (C), 150.2 (C), 190.5 (CO). IR: 3401, 3333 ($\bar{\upsilon}_{NH2}$), 1633 ($\bar{\upsilon}_{C=O}$). HRMS: $[M + H]^+$ calcd for $C_{12}H_{12}NOS$, 218.0640; found, 218.0632.

*1-(5-(3-aminophenyl)thiophen-2-yl)ethanone (**6h**).* Compound **6h** was obtained as a pale yellow powder; R_f 0.30 (PE/EtOAc: 60/40; v/v). ^{1}H NMR (DMSO-d_6) δ: 2.52 (s, 3H, CH_3), 5.31 (s, 2H, NH_2), 6.59 (d, 1H, J = 7.2 Hz), 6.88-6.91 (m, 2H), 7.09 (t, 1H, J = 7.7Hz), 7.46 (d, 1H, J = 4.0Hz), 7.90 (d, 1H, J = 4.0Hz). ^{13}C NMR (DMSO-d_6) δ: 26.3 (CH_3), 110.9 (CH), 113.5 (CH), 114.9 (CH), 124.2 (CH), 129.8 (CH), 133.2 (C-NH_2), 135.1 (CH), 142.0 (C), 149.4 (C), 152.7 (C), 190.5 (CO). IR: 3372, 3218 ($\bar{\upsilon}_{NH2}$), 1642 ($\bar{\upsilon}_{C=O}$). HRMS: $[M + H]^+$ calcd for $C_{12}H_{12}NOS$, 218.0640; found, 218.0641.

*1-(5-(4-aminophenyl)thiophen-2-yl)ethanone (**6i**).* Compound **6i** was obtained as a dark yellow powder; R_f 0.25 (PE/EtOAc: 60/40; v/v). ^{1}H NMR (DMSO-d_6) δ: 2.48 (s, 3H, CH_3), 5.62 (s, 2H, NH_2), 6.60 (d, 2H, J = 8.5Hz), 7.33 (d, 1H, J = 4.0Hz), 7.44 (d, 2H, J = 8.5Hz), 7.83 (d, 1H, J = 4.0Hz). ^{13}C NMR (DMSO-d_6) δ: 26.1 (CH_3), 113.9 (2CH), 120.1 (C-NH_2), 121.5 (CH), 127.2 (2CH), 135.5 (CH), 139.7 (C), 150.3 (C), 153.9 (C), 190.0 (CO). IR: 3327, 3234 ($\bar{\upsilon}_{NH2}$), 1626 ($\bar{\upsilon}_{C=O}$). HRMS: $[M + H]^+$ calcd for $C_{12}H_{12}NOS$, 218.0640; found, 218.0640.

General Synthetic Procedure B for the synthesis of **6d-6f** and **6j-6l**. Compounds **6d-6f**, **6j-6l** and **6s-6t** were prepared according to a procedure described by Bugge et al. or minor modifications thereof.[65] To a solution of the thiophene (2.90 mmol), the corresponding hydroxyphenylboronic acid (2.90 mmol) and $Pd(PPh_3)_4$ (5 mol%) in a mixture of 1,4-dioxane/water (22 mL, 1/1, v/v) was added fine powder K_2CO_3 (11.6 mmol). The reaction was then stirred at 80°C during 6 hours. The cold solution was diluted with ethyl acetate (50 mL), filtered through a Celite pad and the filtrate was diluted with water (60 mL). The aqueous solution was extracted with ethyl acetate (3*50 mL). The organic phases were combined, dried over $MgSO_4$, filtered, and concentrated under reduced pressure to give the crude residue.

*2-(5-nitrothiophen-2-yl)phenol (**6d**).* The crude residue was purified by flash column chromatography (silica gel, CH_2Cl_2/Cyclohexane, 0/100 ramping to 100/0) to give the desired compound. The desired product was dissolved in CH_2Cl_2 (100 mL). The organic phase was washed five times with aqueous solution of NaOH (6 mol.L^{-1}). Then, the aqueous phases were combined, chilled on an ice bath with stirring, acidified to pH 2-3 and extract with CH_2Cl_2 (4*50 mL). The organics phases were combined, dried over $MgSO_4$, filtered, and concentrated under reduced pressure to give **6d** as an orange powder; R_f 0.20 (CH_2Cl_2). ^{1}H NMR (DMSO-d_6) δ: 6.95 (t, 1H, J = 7.6Hz), 7.04 (d, 1H, J = 8.0Hz), 7.28-7.33 (m, 1H), 7.77 (d, 1H, J = 4.6Hz), 7.95 (dd, 1H, J_1 = 8.0Hz, J_2 = 1.1Hz), 8.12 (d, 1H, J = 4.6Hz), 11.32 (br s, 1H, OH).

^{13}C NMR (DMSO-d_6) δ: 116.5 (CH), 118.4 (C-OH), 119.9 (CH), 123.3 (CH), 127.5 (CH), 129.5 (CH), 131.2 (CH), 147.3 (C), 149.4 (C), 154.5 (C). IR: 3433 ($\bar{\upsilon}_{OH}$). HRMS: $[M + H]^+$ calcd for $C_{10}H_8NO_3S$, 222.0225; found, 222.0226.

*3-(5-nitrothiophen-2-yl)phenol (**6e**).* The crude residue was purified by flash column chromatography (silica gel, CH_2Cl_2/Cyclohexane, 0/100 ramping to 100/0) to give the desired compound. The desired product was dissolved in CH_2Cl_2 (100 mL). The organic phase was washed five times with aqueous solution of NaOH (6 mol.L^{-1}). Then, the aqueous phases were combined, chilled on an ice bath with stirring, acidified to pH 2-3 and extract with CH_2Cl_2 (4*50 mL). The organics phases were combined, dried over $MgSO_4$, filtered, and concentrated under reduced pressure to give **6e** as a brown powder; R_f 0.15 (CH_2Cl_2). ^{1}H NMR (DMSO-d_6) δ: 6.88-6.91 (m, 1H), 7.14-7.16 (m, 1H), 7.23-7.33 (m, 2H), 7.60 (d, 1H, J = 4.4Hz), 8.15 (d, 1H, J = 4.4Hz), 9.89 (br s, 1H, OH). ^{13}C NMR (DMSO-d_6) δ: 112.7 (CH), 117.1 (CH), 117.5 (CH), 123.9 (CH), 130.7 (CH), 131.4 (CH), 132.7 (C-OH), 149.1 (C), 151.7 (C), 158.2 (C). IR: 3414 ($\bar{\upsilon}_{OH}$). HRMS: $[M + H]^+$ calcd for $C_{10}H_8NO_3S$, 222.0225; found, 222.0223.

*4-(5-nitrothiophen-2-yl)phenol (**6f**).* The crude residue was purified by flash column chromatography (silica gel, CH_2Cl_2/Cyclohexane, 0/100 ramping to 100/0) to give the desired compound. The desired product was dissolved in CH_2Cl_2 (100 mL). The organic phase was washed five times with aqueous solution of NaOH (6 mol.L^{-1}). Then, the aqueous phases were combined, chilled on an ice bath with stirring, acidified to pH 2-3 and extract with CH_2Cl_2 (4*50 mL). The organics phases were combined, dried over $MgSO_4$, filtered, and concentrated under reduced pressure to give **6f** as a red powder; R_f 0.34 (PE/EtOAc: 80/20; v/v). ^{1}H NMR (DMSO-d_6) δ: 6.87 (d, 2H, J = 8.7Hz), 7.49 (d, 1H, J = 4.4Hz), 7.68 (d, 2H, J = 8.7Hz), 8.11 (d, 1H, J = 4.4Hz), 10.19 (br s, 1H, OH). ^{13}C NMR (DMSO-d_6) δ: 116.3 (2CH), 122.1 (CH), 122.5 (C-OH), 128.1 (2CH), 131.7 (CH), 147.6 (C), 152.9 (C), 159.8 (C). IR: 3342 ($\bar{\upsilon}_{OH}$). HRMS: $[M + H]^+$ calcd for $C_{10}H_8NO_3S$, 222.0225; found, 222.0221.

1-(5-(2-hydroxyphenyl)thiophen-2-yl)ethanone ***(6j)***. The crude residue was purified by flash column chromatography (silica gel, EtOAc/PE, 0/100 ramping to 100/0, v/v) to give the desired compound. The desired product was dissolved in a small amount of ethyl acetate and 150 mL of cold pentane (-20°C) was added, resulting in precipitation of a solid. The solid was filtered, washed twice with 20 mL of cold pentane, and suction-dried to yield **6j** as a beige powder; R_f 0.50 (PE/EtOAc: 60/40; v/v). ^{1}H NMR (DMSO-d_6) δ: 2.52 (s, 3H, CH_3), 6.90 (t, 1H, J = 7.5Hz), 6.99 (d, 1H, J = 7.9Hz), 7.19-7.25 (m, 1H), 7.71 (d, 1H, J = 4.1Hz), 7.77 (dd, 1H, J_1 = 7.8Hz, J_2 = 1.2Hz), 7.88 (d, 1H, J = 4.1Hz), 10.66 (br s, 1H, OH). ^{13}C NMR (DMSO-d_6) δ: 26.5 (CH_3), 116.5 (CH), 119.5 (C), 119.6 (CH), 125.4 (CH), 127.9 (CH), 130.0 (CH), 133.6 (CH), 142.2 (C), 147.7 (C), 154.2 (C), 190.9 (CO). IR: 3168 ($\bar{\upsilon}_{OH}$), 1614 ($\bar{\upsilon}_{C=O}$). HRMS: $[M + H]^+$ calcd for $C_{12}H_{11}O_2S$, 219.0480; found, 219.0480.

1-(5-(3-hydroxyphenyl)thiophen-2-yl)ethanone ***(6k)***. The crude residue was purified by flash column chromatography (silica gel, EtOAC/PE, 0/100 ramping to 100/0, v/v) to give **6k** as a pale yellow powder; R_f 0.50 (PE/EtOAc: 50/50; v/v). ^{1}H NMR (DMSO-d_6) δ: 2.53 (s, 3H, CH_3), 6.80-6.83 (m, 1H), 7.11 (t, 1H, J = 2.0Hz), 7.18-7.29 (m, 2H), 7.56 (d, 1H, J = 4.0Hz), 7.92 (d, 1H, J = 4.0Hz), 9.75 (br s, 1H, OH). ^{13}C NMR (DMSO-d_6) δ: 26.4 (CH_3), 112.6 (CH), 116.3 (CH), 116.9 (CH), 124.9 (CH), 130.4 (CH), 133.9 (C-OH), 135.1 (CH), 142.5 (C), 151.6 (C), 158.0 (C), 190.6 (CO). IR: 3251 ($\bar{\upsilon}_{OH}$), 1619 ($\bar{\upsilon}_{C=O}$). HRMS: $[M + H]^+$ calcd for $C_{12}H_{11}O_2S$, 219.0480; found, 219.0479.

1-(5-(4-hydroxyphenyl)thiophen-2-yl)ethanone ***(6l)***. The crude residue was purified by flash column chromatography (silica gel, PE/EtOAc, 0/100 ramping to 100/0, v/v) to give **6l** as a dark yellow powder; R_f 0.35 (PE/EtOAc: 50/50; v/v). ^{1}H NMR (DMSO-d_6) δ: 2.50 (s, 3H, CH_3), 6.83 (d, 2H, J = 8.6Hz), 7.44 (d, 1H, J = 4.0Hz), 7.59 (d, 2H, J = 8.6Hz), 7.87 (d, 1H, J = 4.0Hz), 9.93 (br s, 1H, OH). ^{13}C NMR (DMSO-d_6) δ: 26.2 (CH_3), 116.0 ($2CH_{AR}$), 123.1 (CH_{AR}), 123.8 (C-OH), 127.6 ($2CH_{AR}$), 135.3 (CH_{AR}), 141.1 (C), 152.4 (C), 158.6 (C), 190.3

(CO). IR: 3117 ($\bar{\upsilon}_{OH}$), 1600 ($\bar{\upsilon}_{C=O}$). HRMS: $[M + H]^+$ calcd for $C_{12}H_{11}O_2S$, 219.0480; found, 219.0481.

General Synthetic Procedure C for the synthesis of **6m-6o**. Compounds **6m-6o** and **6u** were prepared according to a procedure described by Valant et al. or minor modifications thereof.[66] To a solution of **3** (1.82 mmol), the corresponding aminophenylboronic acid (HCl salt) (3.64 mmol) and $Pd[PPh_3]_2Cl_2$ (10 mol%) in DMF (14 mL) was added 2M aqueous potassium carbonate (3.7 mL). The mixture was heated to 70°C during 1 hour. The cold solution was diluted with ethyl acetate (50 mL), filtered through a Celite pad and the filtrate was diluted with water (60 mL). The aqueous solution was extracted with ethyl acetate (3*50 mL). The organic phases were combined, washed with brine (8*40 mL), dried over $MgSO_4$, filtered, and concentrated under reduced pressure to give the crude compound. The residue was purified by flash column chromatography (silica gel, EtOAC/PE, 25/75 ramping to 100/0, v/v) to give the desired compound.

*N-(5-(2-aminophenyl)thiophen-2-yl)acetamide (**6m**).* Compound **6m** was obtained as a brown powder; R_f 0.20 (PE/EtOAc: 40/60; v/v). ^{1}H NMR (DMSO-d_6) δ: 2.07 (s, 3H, CH_3), 4.98 (s, 2H, NH_2), 6.56-6.63 (m, 2H), 6.75 (dd, 1H, J_1 = 8.0Hz, J_2 = 1.0Hz), 6.94-7.02 (m, 2H), 7.10 (dd, 1H, J_1 = 7.6Hz, J_2 = 1.4Hz), 11.13 (br s, 1H, OH). ^{13}C NMR (DMSO-d_6) δ: 22.5 (CH_3), 110.8 (CH_{AR}), 115.6 (CH_{AR}), 116.7 (CH_{AR}), 118.8 (C), 122.1 (CH_{AR}), 128.0 (CH_{AR}), 129.6 (CH_{AR}), 131.2 (C), 139.0 (C), 145.4 (C), 166.2 (CO). IR: 3462, 3370 ($\bar{\upsilon}_{NH2}$), 3234 ($\bar{\upsilon}_{NH}$), 1570 ($\bar{\upsilon}_{C=O}$). HRMS: $[M + H]^+$ calcd for $C_{12}H_{13}N_2OS$, 233.0749; found, 233.0745.

*N-(5-(3-aminophenyl)thiophen-2-yl)acetamide (**6n**).* Compound **6n** was obtained as a white powder; R_f 0.20 (PE/EtOAc: 30/70; v/v). ^{1}H NMR (DMSO-d_6) δ: 2.07 (s, 3H, CH_3), 5.12 (s, 2H, NH_2), 6.42 (dd, 1H, H_{AR}, J_1 = 7.9Hz, J_2 = 1.1Hz), 6.57 (d, 1H, H_{AR}, J = 3.9Hz), 6.71-6.76 (m, 2H, H_{AR}), 6.99 (t, 1H, H_{AR}, J = 7.8Hz), 7.05 (d, 1H, H_{AR}, J = 3.9Hz), 11.14 (s, 1H, NH). ^{13}C NMR (DMSO-d_6) δ: 22.5 (CH_3), 110.0 (CH_{AR}), 111.1 (CH_{AR}), 112.4 (CH_{AR}), 112.5

(CH_{AR}), 119.6 (CH_{AR}), 129.4 (CH_{AR}), 134.1 (C), 134.8 (C), 138.9 (C), 149.1 (C), 166.2 (CO). IR: 3469, 3372 ($\bar{\upsilon}_{NH2}$), 3274 ($\bar{\upsilon}_{NH}$), 1562 ($\bar{\upsilon}_{C=O}$). HRMS: $[M + H]^+$ calcd for $C_{12}H_{13}N_2OS$, 233.0749; found, 233.0749.

*N-(5-(4-aminophenyl)thiophen-2-yl)acetamide (**6o**).* Compound **6o** was obtained as a beige powder; R_f 0.15 (PE/EtOAc: 30/70; v/v). ^{1}H NMR (DMSO-d_6) δ: 2.05 (s, 3H, CH_3), 5.57 (s, 2H, NH_2), 6.52 (d, 1H, J = 3.9Hz), 6.60 (d, 2H, J = 8.5Hz), 6.90 (d, 1H, J = 3.9Hz), 7.24 (d, 2H, J = 8.5Hz), 11.04 (br s, 1H, NH). ^{13}C NMR (DMSO-d_6) δ: 22.5 (CH_3), 111.2 (CH), 114.7(2CH), 117.3 (CH), 122.9 (C), 125.6 (2CH), 134.7 (C), 137.3 (C), 146.8 (C), 166.0 (CO). IR: 3388, 3321 ($\bar{\upsilon}_{NH2}$), 3181 ($\bar{\upsilon}_{NH}$), 1581 ($\bar{\upsilon}_{C=O}$). HRMS: $[M + H]^+$ calcd for $C_{12}H_{13}N_2OS$, 233.0749; found, 233.0754.

General Synthetic Procedure D for the synthesis of **6p-6r.** Compounds **6p-6r** were prepared according to a procedure described by Ashwell et al. or minor modifications thereof.[67] To a solution of **3** (4.54 mmol), the corresponding hydroxyphenylboronic acid (9.08 mmol) and $Pd[PPh_3]_2Cl_2$ (10 mol%) in DMF (34 mL) was added fine powder of cesium carbonate (18.2 mmol) and water (10mL). The mixture was heated to 80°C during 3 hours. The cold solution was diluted with ethyl acetate (50 mL), filtered through a Celite pad and the filtrate was diluted with water (80 mL). The aqueous solution was extracted with ethyl acetate (3*80 mL). The organic phases were combined, washed with brine (12*50 mL), dried over $MgSO_4$, filtered, and concentrated under reduced pressure to give the crude compound. The residue was purified by flash column chromatography (silica gel, EtOAC/PE, 25/75 ramping to 100/0, v/v) to give the desired compound.

*N-(5-(2-hydroxyphenyl)thiophen-2-yl)acetamide (**6p**).* Compound **6p** was obtained as a beige powder; R_f 0.45 (PE/EtOAc: 20/80; v/v). ^{1}H NMR (DMSO-d_6) δ: 2.06 (s, 3H, CH_3), 6.60 (d, 1H, H_{AR}, J = 4.0Hz), 6.78-6.83 (m, 1H, H_{AR}), 6.90 (dd, 1H, J_1 = 8.1Hz, J_2 = 1.1Hz), 7.01-7.06 (m, 1H), 7.31 (d, 1H, J = 4.0Hz), 7.52 (dd, 1H, J_1 = 7.8Hz, J_2 = 1.6Hz), 9.99 (br s,

1H, OH), 11.04 (br s, 1H, NH). ^{13}C NMR (DMSO-d_6) δ: 22.6 (CH_3), 110.4 (CH), 116.1 (CH), 119.4 (CH), 121.3 (C), 121.7 (CH), 126.9 (CH), 127.2 (CH), 129.9 (C), 140.0 (C), 153.0 (C), 166.1 (CO). IR: 3073 ($\bar{\upsilon}_{OH}$), 1563 ($\bar{\upsilon}_{C=O}$). HRMS: $[M + H]^+$ calcd for $C_{12}H_{12}NO_2S$, 234.0589; found, 233.0588.

*N-(5-(3-hydroxyphenyl)thiophen-2-yl)acetamide (**6q**).* Compound **6q** was obtained as a beige powder; R_f 0.35 (PE/EtOAc: 20/80; v/v). ^{1}H NMR (DMSO-d_6) δ: 2.07 (s, 3H, CH_3), 6.58 (d, 1H, J = 3.9Hz), 6.63 (dd, 1H, J_1 = 7.7Hz, J_2 = 2.0Hz), 6.94 (t, 1H, J = 1.9Hz), 6.99 (d, 1H, J = 8.0Hz), 7.12-7.18 (m, 2H), 9.46 (br s, 1H, OH), 11.20 (br s, 1H, NH). ^{13}C NMR (DMSO-d_6) δ: 22.5 (CH_3), 112.2 (2CH), 113.7 (CH), 115.5 (CH), 120.3 (CH), 130.0 (CH), 133.1 (C), 135.6 (C), 139.4 (C), 157.8 (C), 166.3 (CO). IR: 3248 ($\bar{\upsilon}_{OH}$), 1576 ($\bar{\upsilon}_{C=O}$). HRMS: $[M + H]^+$ calcd for $C_{12}H_{12}NO_2S$, 234.0589; found, 233.0590.

*N-(5-(4-hydroxyphenyl)thiophen-2-yl)acetamide (**6r**).* Compound **6r** was obtained as a pale purple powder; R_f 0.50 (PE/EtOAc: 10/90; v/v). ^{1}H NMR (DMSO-d_6) δ: 2.06 (s, 3H, CH_3), 6.54 (d, 1H, J = 3.9Hz), 6.76 (d, 2H, J = 8.6Hz), 6.99 (d, 1H, J = 3.9Hz), 7.35 (d, 2H, J = 8.6Hz), 9.49 (br s, 1H, OH), 11.09 (br s, 1H, NH). ^{13}C NMR (DMSO-d_6) δ: 22.5 (CH_3), 111.2 (CH), 115.8 (2CH), 118.5 (CH), 125.5 (C), 126.0 (2CH), 133.8 (C), 138.1 (C), 156.5 (C), 166.1 (CO). IR: 3266 ($\bar{\upsilon}_{OH}$), 1574 ($\bar{\upsilon}_{C=O}$). HRMS: $[M + H]^+$ calcd for $C_{12}H_{12}NO_2S$, 234.0589; found, 233.0589.

*2-(2,3-dimethoxyphenyl)-5-nitrothiophene (**6s**).* To a solution of **1** (5.49 mmol), 2,3-Dimethoxyphenyl boronic acid (5.49 mmol) and $Pd(PPh_3)_4$ (5 mol%) in 1,4-dioxane (23 mL) was added potassium carbonate (22 mmol) and water (23 mL). The mixture was heated to 80°C during 6 hours. The cold solution was diluted with ethyl acetate (50 mL), filtered through a Celite pad and the filtrate was diluted with water (80 mL). The aqueous solution was extracted with ethyl acetate (3*80 mL). The organic phases were combined, dried over $MgSO_4$, filtered, and concentrated under reduced pressure to give the crude compound. The

residue was purified by flash column chromatography (silica gel, CH_2Cl_2/cyclohexane, 0/100 ramping to 100/0) to give **6s** as a yellow powder; R_f 0.40 (PE/EtOAc: 80/20; v/v). ^{1}H NMR (DMSO-d_6) δ: 3.88 (s, 3H, OCH_3), 3.89 (s, 3H, OCH_3), 7.15-7.24 (m, 2H, $2H_{AR}$), 7.61 (dd, 1H, H_{AR}, J_1 = 7.2Hz, J_2 = 2.3Hz), 7.80 (d, 1H, H_{AR}, J = 4.6Hz), 8.14 (d, 1H, H_{AR}, J = 4.6Hz). ^{13}C NMR (DMSO-d_6) δ: 56.0 (OCH_3), 59.9 (OCH_3), 114.3 (CH), 118.8 (CH), 124.7 (C), 124.8 (CH), 125.0 (CH), 129.6 (CH), 145.3 (C), 145.4 (C), 150.5 (C), 152.8 (C). IR: 1258 ($\bar{\upsilon}_{C-O}$). HRMS: $[M + H]^+$ calcd for $C_{12}H_{12}NO_4S$, 266.0487, found 266.0486.

*1-(5-(2,3-dimethoxyphenyl)thiophen-2-yl)ethanone (**6t**).* To a solution of **2** (5.49 mmol), 2,3-Dimethoxyphenyl boronic acid (5.49 mmol) and $Pd(PPh_3)_4$ (5 mol%) in 1,4-dioxane (23 mL) was added potassium carbonate (22 mmol) and water (23 mL). The mixture was heated to 80°C during 16 hours. The cold solution was diluted with ethyl acetate (50 mL), filtered through a Celite pad and the filtrate was diluted with water (80 mL). The aqueous solution was extracted with ethyl acetate (4*80 mL). The organic phases were combined, dried over $MgSO_4$, filtered and concentrated under reduced pressure to give the crude compound. The residue was purified by flash column chromatography (silica gel, EtOAC/PE, 0/100 ramping to 100/0, v/v) to give **6t** as a pale yellow powder; R_f 0.31 (PE/EtOAc: 80/20; v/v). ^{1}H NMR (DMSO-d_6) δ: 2.54 (s, 3H, CH_3), 3.79 (s, 3H, OCH_3), 3.86 (s, 3H, OCH_3), 7.08-7.19 (m, 2H), 7.46 (dd, 1H, J_1 = 7.8Hz, J_2 = 1.6Hz), 7.71 (d, 1H, J = 4.1Hz), 7.91 (d, 1H, J = 4.1Hz). ^{13}C NMR (DMSO-d_6) δ: 26.6 (CH_3), 55.9 (OCH_3), 59.8 (OCH_3), 113.3 (CH), 119.3 (CH), 124.6 (CH), 126.1 (C), 126.6 (CH), 133.5 (CH), 143.5 (C), 145.3 (C), 145.8 (C), 153.1 (C), 191.1 (CO). IR: 1644 ($\bar{\upsilon}_{C=O}$), 1259 ($\bar{\upsilon}_{C-O}$). HRMS: $[M + H]^+$ calcd for $C_{14}H_{15}O_3S$, 263.0742, found 263.0741.

*N-(5-(2,3-dimethoxyphenyl)thiophen-2-yl)acetamide (**6u**).* To a solution of **3** (1.59 mmol), 2,3-Dimethoxyphenyl boronic acid (3.18 mmol) and $Pd[PPh_3]_2Cl_2$ (10 mol%) in DMF (12 mL) was added fine powder of potassium carbonate (6.36 mmol) and water (3.5 mL). The

mixture was heated to 80°C during 3 hours. The cold solution was diluted with ethyl acetate (50 mL), filtered through a Celite pad and the filtrate was diluted with water (50 mL). The aqueous solution was extracted with ethyl acetate (4*50 mL). The organic phases were combined, washed with brine (6*40 mL), dried over $MgSO_4$, filtered, and concentrated under reduced pressure to give the crude compound. The residue was purified by flash column chromatography (silica gel, EtOAC/PE, 10/90 ramping to 100/0, v/v) to give **6u** as a beige powder; R_f 0.30 (PE/EtOAc: 40/60; v/v). ^{1}H NMR (DMSO-d_6) δ: 2.07 (s, 3H, CH_3), 3.71 (s, 3H, OCH_3), 3.83 (s, 3H, OCH_3), 6.62 (d, 1H, J = 4.0Hz), 6.91 (dd, 1H, J_1 = 8.1Hz, J_2 = 1.1Hz), 7.06 (t, 1H, J = 8.1Hz), 7.25 (dd, 1H, J_1 =8.0Hz, J_2 = 1.3Hz), 7.31 (d, 1H, J = 4.0Hz), 11.12 (br s, 1H, NH). ^{13}C NMR (DMSO-d_6) δ: 22.6 (CH_3), 55.8 (OCH_3), 59.6 (OCH_3), 110.4 (CH), 110.7 (CH), 118.5 (CH), 122.7 (CH), 124.4 (CH), 127.9 (C), 128.1 (C), 141.5 (C), 144.2 (C), 153.2 (C), 166.2 (CO). IR: 3211 ($\bar{\upsilon}_{NH}$), 1569 ($\bar{\upsilon}_{C=O}$), 1302 ($\bar{\upsilon}_{C-O}$). HRMS: $[M + H]^+$ calcd for $C_{14}H_{16}NO_3S$, 278.0851, found 278.0849.

General Synthetic Procedure E for the synthesis of **7a-7c.** Compounds **7a-7c** were prepared according to a procedure described by Bhanu Prasad and Gilbertson or minor modifications thereof.[68] A solution of **6a-6c** (2.72 mmol) and 2-iodoethanol (27.2 mmol) was heated to 90°C under nitrogen atmosphere in a sealed tube during 3 hours. The cold solution was diluted with ethyl acetate (100 mL), washed with 2M aqueous solution of NaOH (3*30 mL), brine solution (3*30 mL), dried over $MgSO_4$, filtered and concentrated under reduced pressure to give the crude compound. The residue was purified by flash column chromatography (silica gel, EtOAC/PE, 10/90 ramping to 100/0, v/v) to give the desired compound.

*2-((2-(5-nitrothiophen-2-yl)phenyl)amino)ethanol (**7a**).* Compound **7a** was obtained as a red powder; R_f 0.25 (PE/EtOAc: 40/60; v/v). ^{1}H NMR (DMSO-d_6) δ: 3.16 (q, 2H, CH_2O, J = 5.8Hz), 3.59 (q, 2H, CH_2N, J = 5.5Hz), 4.79 (t, 1H, OH, J = 5.3Hz), 5.32 (t, 1H, NH, J = 5.5Hz), 6.73 (t, 1H, J_1 = 7.4Hz), 6.82 (d, 1H, J = 8.1Hz), 7.26-7.33 (m, 2H), 7.42 (d, 1H, J =

4.3Hz), 8.18 (d, 1H, *J* = 4.3Hz). ^{13}C NMR (DMSO-d_6) δ: 45.7 (CH_2O), 59.1 (CH_2N), 112.1 (CH), 117.0 (CH), 117.4 (C-N), 126.3 (CH), 130.6 (CH), 130.8 (CH), 131.3 (CH), 146.1 (C), 149.0 (C), 150.0 (C). IR: 3214 ($\bar{\upsilon}_{OH}$). HRMS: $[M + H]^+$ calcd for $C_{12}H_{13}N_2O_3S$, 265.0647, found 265.0645.

*2-((3-(5-nitrothiophen-2-yl)phenyl)amino)ethanol (**7b**).* Compound **7b** was obtained as a red powder; R_f 0.50 (PE/EtOAc: 30/70; v/v). ^{1}H NMR (DMSO-d_6) δ: 3.16 (q, 2H, CH_2O, *J* = 5.7Hz), 3.58 (q, 2H, CH_2N, *J* = 5.7Hz), 4.72 (t, 1H, OH, *J* = 5.4Hz), 5.86 (t, 1H, NH, *J* = 5.3Hz), 6.71 (d, 1H, *J* = 8.7Hz), 6.95-6.97 (m, 2H), 7.18 (t, 1H, *J* = 7.9Hz), 7.55 (d, 1H, *J* = 4.3Hz), 8.13 (d, 1H, *J* = 4.3Hz). ^{13}C NMR (DMSO-d_6) δ: 45.3 (CH_2O), 59.6 (CH_2N), 108.8 (CH), 113.5 (CH), 114.3 (CH), 123.4 (CH), 130.0 (CH), 131.3 (CH), 132.0 (C-N), 148.7 (C), 149.7 (C), 153.0 (C). IR: 3274, 3113 ($\bar{\upsilon}_{NH}$), 3179 ($\bar{\upsilon}_{OH}$). HRMS: $[M + H]^+$ calcd for $C_{12}H_{13}N_2O_3S$, 265.0647, found 265.0648.

*2-((4-(5-nitrothiophen-2-yl)phenyl)amino)ethanol (**7c**).* Compound **7c** was obtained as a dark red powder; R_f 0.35 (PE/EtOAc: 10/90; v/v). ^{1}H NMR (DMSO-d_6) δ: 3.17 (q, 2H, CH_2O, *J* = 5.8Hz), 3.56 (q, 2H, CH_2N, *J* = 5.8Hz), 4.77 (t, 1H, OH, *J* = 5.4Hz), 6.47 (t, 1H, NH, *J* = 5.6Hz), 6.66 (d, 2H, *J* = 8.8Hz), 7.38 (d, 1H, *J* = 4.5Hz), 7.57 (d, 2H, *J* = 8.7Hz), 8.06 (d, 1H, *J* = 4.5Hz). ^{13}C NMR (DMSO-d_6) δ: 45.1 (CH_2O), 59.5 (CH_2N), 112.1 (2CH), 118.4 (C-N), 120.4 (CH), 127.7 (2CH), 132.1 (CH), 145.7 (C), 151.2 (C), 154.8 (C). IR: 3310 ($\bar{\upsilon}_{OH}$). HRMS: $[M + H]^+$ calcd for $C_{12}H_{13}N_2O_3S$, 265.0647, found 265.0644.

General Synthetic Procedure F for the synthesis of **8a, 8c, 8e-8i**. To a cold solution (ice bath) of the corresponding amine (2.11 mmol) in THF (10 mL) was added dropwise 10 mL of concd. HCl solution (37%, c=12 mol.L^{-1}) resulting in precipitation of a solid from the first drop. The solution was stirred at 0°C during 20 minutes. The solid was filtered by suction on filter funnel (porosity 4), washed three times with 20 mL of cold pentane (-20 °C) to afford the desired product.

*2-(5-nitrothiophen-2-yl)aniline hydrochloride (**8a**).* Compound **8a** was obtained as a pale red powder in 37% yield. ^{1}H NMR (DMSO-d_6) δ: 6.79 (br s, 3H, NH_3^+), 7.00 (t, 1H, J = 7.5Hz), 7.16-7.19 (m, 1H), 7.34 (t, 1H, J = 8.3Hz), 7.45 (dd, 1H, J = 7.7Hz, J = 1.3Hz), 7.55 (d, 1H, J = 4.3Hz), 8.18 (d, 1H, J = 4.3Hz). ^{13}C NMR (DMSO-d_6) δ: 121.0 (CH), 121.4 (C), 122.9 (CH), 127.1 (CH), 130.7 (CH), 130.8 (CH), 131.0 (CH), 138.4 (C), 148.2 (C), 149.8 (C). IR: 2797 ($\bar{\upsilon}_{NH3+}$). HRMS: $[M + H]^+$ calcd for $C_{10}H_9N_2O_2S$, 221.0385, found 221.0386.

*4-(5-nitrothiophen-2-yl)aniline hydrochloride (**8c**).* Compound **8c** was obtained as a brown powder in 59% yield. ^{1}H NMR (DMSO-d_6) δ: 7.11 (d, 2H, J = 8.6Hz), 7.54 (d, 1H, J = 4.4Hz), 7.76 (d, 2H, J = 8.6Hz), 8.12 (d, 1H, J = 4.4Hz), 8.54 (br s, 3H, NH_3^+). ^{13}C NMR (DMSO-d_6) δ: 120.5 (2CH), 123.1 (CH), 126.4 (C), 127.7 (2CH), 131.6 (CH), 140.4 (C), 148.3 (C), 151.8 (C). IR: 2808 ($\bar{\upsilon}_{NH3+}$). HRMS: $[M + H]^+$ calcd for $C_{10}H_9N_2O_2S$, 221.0385, found 221.0384.

*1-(5-(3-aminophenyl)thiophen-2-yl)ethanone hydrochloride (**8e**).* Compound **8e** was obtained as a pale yellow powder in 35% yield. ^{1}H NMR (DMSO-d_6) δ: 2.55 (s, 3H, CH_3), 7.29 (d, 1H, , J = 8Hz), 7.51 (t, 1H, J = 7.9Hz), 7.62-7.69 (m, 3H), 7.97 (d, 1H, J = 4Hz) (The signal for NH_3^+ is not visible). ^{13}C NMR (DMSO-d_6) δ: 26.4 (CH_3), 119.0 (CH), 122.4 (CH), 123.5 (CH), 125.7 (CH), 130.7 (CH), 133.9 (C), 135.2 (CH), 135.8 (C), 143.3 (C), 145.0 (C), 190.8 (CO). IR: 2779 ($\bar{\upsilon}_{NH3+}$), 1618 ($\bar{\upsilon}_{C=O}$). HRMS: $[M + H]^+$ calcd for $C_{12}H_{12}NOS$, 218.0640, found 218.0641.

*1-(5-(4-aminophenyl)thiophen-2-yl)ethanone hydrochloride (**8f**).* Compound **8f** was obtained as a pale brown powder in 39% yield. ^{1}H NMR (DMSO-d_6) δ: 2.53 (s, 3H, CH_3), 7.31 (d, 2H, J = 8.5Hz), 7.60 (d, 1H, J = 4.0Hz), 7.80 (d, 2H, J = 8.5Hz), 7.94 (d, 2H, J = 8.5Hz), 8.93 (br s, 3H, NH_3^+). ^{13}C NMR (DMSO-d_6) δ: 26.3 (CH_3), 122.1 (2CH), 124.9 (CH), 127.2 (2CH), 129.9 (C), 135.2 (CH), 136.1 (C), 142.6 (C), 150.6 (C), 190.5 (CO). IR: 2883 ($\bar{\upsilon}_{NH3+}$), 1653 ($\bar{\upsilon}_{C=O}$). HRMS: $[M + H]^+$ calcd for $C_{12}H_{12}NOS$, 218.0640, found 218.0640.

N-(5-(2-aminophenyl)thiophen-2-yl)acetamide hydrochloride (**8g**). Compound **8g** was obtained as a white powder in 49% yield. ^{1}H NMR (DMSO-d_6) δ: 2.10 (s, 3H, CH_3), 6.72 (d, 1H, J = 3.9Hz), 7.33-7.40 (m, 3H), 7.44-7.52 (m, 2H), 9.32 (br s, 3H, NH_3^+), 11.56 (s, 1H, NH). ^{13}C NMR (DMSO-d_6) δ: 22.4 (CH_3), 111.2 (CH), 123.5 (CH), 124.8 (CH), 127.1 (CH), 127.5 (2C), 128.1 (CH), 130.5 (CH), 131.1 (C), 141.2 (C), 166.5 (CO). IR: 2803 ($\bar{\upsilon}_{NH3+}$), 1571($\bar{\upsilon}_{C=O}$). HRMS: $[M + H]^+$ calcd for $C_{12}H_{13}N_2OS$, 233.0749, found 233.0752.

N-(5-(3-aminophenyl)thiophen-2-yl)acetamide hydrochloride (**8h**). Compound **8h** was obtained as a pink powder in 46% yield. ^{1}H NMR (DMSO-d_6) δ: 2.10 (s, 3H, CH_3), 6.66 (d, 1H, J = 4Hz), 7.16 (d, 1H, J = 7.8Hz), 7.27 (d, 1H, J = 4Hz), 7.41-7.48 (m, 2H), 7.56 (d, 1H, J = 7.8Hz), 11.47 (s, 1H) (The signal for NH_3^+ is not visible). ^{13}C NMR (DMSO-d_6) δ: 22.5 (CH_3), 111.5 (CH), 118.1 (CH), 120.2 (CH), 121.6 (CH), 122.9 (CH), 130.3 (CH), 131.4 (C), 134.1 (C), 135.8 (C), 140.4 (C), 166.5 (CO). IR: 2865 ($\bar{\upsilon}_{NH3+}$), 1571 ($\bar{\upsilon}_{C=O}$). HRMS: $[M + H]^+$ calcd for $C_{12}H_{13}N_2OS$, 233.0749, found 233.0751.

N-(5-(4-aminophenyl)thiophen-2-yl)acetamide hydrochloride (**8i**). Compound **8i** was obtained as a beige powder in 51% yield. ^{1}H NMR (DMSO-d_6) δ: 2.09 (s, 3H, CH_3), 6.65 (d, 1H, J = 4.0Hz), 7.27 (d, 1H, J = 4.0Hz), 7.36 (d, 2H, J = 8.5Hz), 7.66 (d, 2H, J = 8.5Hz), 10.29 (br s, 3H, NH_3^+), 11.48 (s, 1H, NH). ^{13}C NMR (DMSO-d_6) δ: 22.5 (CH_3), 116.5 (CH), 121.4 (CH), 123.7 (2CH), 125.5 (2CH), 130.3 (C), 131.6 (C), 134.1 (C), 140.2 (C), 166.4 (CO). IR: 2816 ($\bar{\upsilon}_{NH3+}$), 1564 ($\bar{\upsilon}_{C=O}$). HRMS: $[M + H]^+$ calcd for $C_{12}H_{13}N_2OS$, 233.0749, found 233.0747.

3-(5-nitrothiophen-2-yl)aniline hydrochloride (**8b**). Hydrochloric acid gas was formed by the slowly addition of concd. solution of sulfuric acid (97%, 15 mL) to NaCl (40 g). This gas was cannulated in a cold solution (ice bath) of **6b** (2.37 mmol) in THF (10 mL) during 20 minutes resulting in precipitation of a solid. The solution was filtered by suction on filter funnel (porosity 4), washed three times with 20 mL of a cold pentane (-20 °C) to give **8b** as a

green powder in 89% yield. ^{1}H NMR (DMSO-d_6) δ: 7.36 (dd, 1H, J = 8.0Hz, J = 1.1Hz), 7.54 (t, 1H, J = **7**.9Hz), 7.64-7.73 (m, 3H), 8.18 (d, 1H, J = 4.4Hz), 9.09 (br s, 3H, NH_3^+). ^{13}C NMR (DMSO-d_6) δ: 118.9 (CH), 123.2 (CH), 123.5 (CH), 124.6 (CH), 130.8 (CH), 131.3 (CH), 132.6 (C), 136.4 (C), 149.7 (C), 150.1 (C). IR: 2816 ($\bar{\upsilon}_{NH3+}$). HRMS: $[M + H]^+$ calcd for $C_{10}H_9N_2O_2S$, 221.0385, found 221.0385.

1-(5-(2-aminophenyl)thiophen-2-yl)ethanone hydrochloride (**8d**). To a cold solution (ice bath) of **6g** (1.81 mmol) in 8 mL of THF was added dropwise 18 mL of concd. HCl solution (37%, c=12 mol.L^{-1}). The solution was stirred at 0°C during 20 minutes. The solvent was evaporated under reduce pressure. 25 mL of diethylether was added and the solution was concentrated under reduce pressure. This operation was repeated ten times resulting in formation of **8d** as a brown solid in 96% yield. ^{1}H NMR (DMSO-d_6) δ: 2.56 (s, 3H, CH_3), 7.17 (t, 1H, J = **7**.0Hz), 7.33-7.42 (m, 2H), 7.47 (d, 1H, J = 7.5Hz), 7.62 (d, 1H, J = 3.9Hz), 8.00 (d, 1H, J = 3.9Hz), 8.27 (br s, 3H, NH_3^+). ^{13}C NMR (DMSO-d_6) δ: 26.5 (CH_3), 122.9 (C), 125.5 (CH), 125.9 (C), 128.9 (CH), 130.2 (CH), 131.1 (CH), 133.4 (C), 134.7 (CH), 144.2 (C), 146.7 (CH), 190.8 (CO). IR: 2714 ($\bar{\upsilon}_{NH3+}$), 1623 ($\bar{\upsilon}_{C=O}$). HRMS: $[M + H]^+$ calcd for $C_{12}H_{12}NOS$, 218.0640, found 218.0641.

4.3. Bacterial strains and growth conditions

All bacteria used in this study were cultivated according to 'American Type Culture Collection (ATCC) guidelines (www.atcc.org). *Bacillus subtilis* JH642, *Bacillus anthracis* 34F2, *Salmonella enterica* 14028s and *Escherichia coli* MG1655 were grown in lysogeny broth (LB). Tryptic soy broth (TSA) was used for the cultivation of *Staphylococcus aureus* TCH1516 USA300. *Streptococcus pyogenes* GAS M1 5448, *Streptococcus agalactiae* GBS CoH1, *Listeria monocytogenes* 10403s and *Enterococcus faecalis* V583 were grown in brain

heart infusion broth (BHI). For plating the bacteria 1.7% agar was added to the respective broth. All bacteria were routinely grown at 30 or 37 °C under agitation at 200 rpm. For *E. coli* protein expression strain BL21 (DE3) was used and a final concentration of 100 µg/ml ampicillin and 50 µg/ml kanamycin were utilized to maintain expression plasmids.

4.3.1 Construction of kinase expression plasmids

To construct expression strains for cytoplasmic fragments of *B. subtilis* histidine kinases PhoR and ResE, *B. subtilis* stain JH642 genomic DNA was subjected to PCR amplification with the following two primer pairs:

phoRf-5'-GAGTCAGCTAGCAATGTAGCCACAGAAC-3'/phoRr-5'-CCTTTGGGATCCTTAGGCGGACTTTTC-3'

resEf-5'-CTCCGACATATGAGAGAAGGCGCG-3'/resEr-5'-GGAACAGGATCCTTCGGCAAATTCAGAC-3'

The two corresponding PCR products encode entire cytoplasmic fragments for PhoR (residues 186-589) and ResE (residues 203-589). The DNA fragments were cloned into NheI and BamHI (PhoR) or NdeI and BamHI (ResE) sites of vector pET28a resulting in vectors pET-PhoR and pET-ResE. These vectors are capable of expressing hexa-his-tagged recombinant soluble proteins fragment of PhoR and ResE, respectively.

4.3.2 Purification of His- tagged proteins

Hexa-his-tagged PhoR, ResE and IreK were purified from *E. coli* BL21(DE3) carrying the respective plasmids pET-PhoR, pET-ResE and pCJK111.[69] Starter cultures were grown in 25 ml LB for 12-16h. 1 l LB was inoculated to an optical density at 600 nm (OD_{600}) of 0.05. When cultures reached an OD_{600} of 0.6 the temperature was shifted to 16 °C and protein expression was induced by the addition of 1 mM IPTG. Protein expression was allowed to

continue for 12-15h. Cells were harvested, suspended in 5x (w/v) buffer A (50 mM Tris and 200 mM NaCl) and crude lysates were prepared by passage through a French pressure cell. The cell lysates were cleared of cell debris by centrifugation (at 6000xg for 20 min and 4 °C and at 80000xg for 1 h at 4 °C). The cleared supernatant was incubated with Ni-NTA agarose (Qiagen) for 12-16h at 4 °C. Following an initial wash step with buffer A, the proteins were eluted with the same buffer containing 250 mM imidazole and dialyzed against buffer A. To verify the successful purification of the respective protein samples were analyzed by SDS-polyacrylamide gel electrophoresis. Other purified proteins utilized here were kind gifts from other labs. *B. subtilis* $WalK^{204-612}$ was a gift from Marta Perego, $WalK^{272-616}$ was a gift from Liang Tang.

4.3.3 Kinase assay and IC_{50} determination

Autophosphorylation assays of histidine kinases (PhoR, ResE and WalK) and serine/threonine kinase (IreK) were performed similar to a previously described assay of Igarashi *et al.*[70] Briefly, for initial inhibition screens, a 20 µl reaction contained 4 µl 5x kinase reaction buffer (250 mM Epps, 100 mM $MgCl_2$, 0.5 mM EDTA, 25% glycerol, pH 8.5) and 2 µM of the respective kinase. Putative histidine kinase inhibitors dissolved in DMSO were added to the reactions to a final concentration of 1mM and all reactions contained a final concentration of 10% DMSO. Following a 5 min exposure ATP was added to the reaction mixture to a final concentration of 1 mM (0.3125 µM [γ-^{32} ATP] and ~ 1 mM ATP). The reaction was stopped by addition of 5x SDS-PAGE loading buffer (300mM Tris/HCl pH6.8, 50% glycerol, 10% SDS, 25% **β**-mercaptoetanol, 0.05% bromphenol blue). The samples were subjected to SDS-PAGE immediately after inactivation. SDS-PAGE gels were exposed to an imaging plate for approximately 15 h. The scanner Typhoon FLA 7000 (GE Healtcare Life Sciences) was used for the detection of radiolabeled kinases. For evaluation of the signal intensity and determination of IC_{50} values the software ImageJ (NIH) and GraphPad Prism 6 (Graph Pad

Software) were used. For IC_{50} determination, as described by Igarashi et al. [70], the assay was modified by dropping kinase concentration to 0.5 μM and ATP to a final concentration of 2.5 μM. The ratio of cold and hot ATP had to be determined empirically for each kinase to allow for proper signal detection and was 1:1 for PhoR, 1:10 for ResE and 1:4 for WalK. Compounds were added to final concentrations of 0, 6.25, 12.5, 25, 50, 100, 200, 400 and 800 μM prior to addition of ATP and keeping DMSO concentrations constant.

4.3.4 Gyrase assay

E. coli gyrase (catalog # M0306S) and its substrate (pUC19; catalog # N0471S) were purchased from NEB. The gyrase catalyzed supercoiling reaction was set up according to the manufacturer. Briefly, each reaction contained 1 Unit gyrase, 75 ng substrate, 2% DMSO and 3 μl of gyrase buffer (NEB) in a final volume of 15 μl. When appropriate the compound solution was added to the reaction mixture to obtain a final concentration of 6.25; 12.5; 25; 50; 100; 200; 400 and 800 μM of the respective compound keeping DMSO concentrations constant. Ciprofloxacin, a known gyrase inhibitor was used as control and added to the reaction mixture to a final concentration of 200 μM. The samples were incubated for 30 minutes at 37 °C. Afterwards the reaction was stopped with DNA Loading Dye. The samples were analyzed by agarose gel electrophoresis immediately after inactivation

4.3.5 Determination of the antimicrobial activity of the compounds

The antimicrobial activity of all compounds were evaluated *in vitro* against seven reference Gram-positive and two Gram-negative bacteria (see ***Bacterial strains and growth conditions***) utilizing the following two assays.

4.3.6 Disk Diffusion Assay

The Kirby-Bauer disk diffusion susceptibility assay was used to determine the sensitivity of bacteria to selected compounds according to the 'Clinical Laboratory Standards Institute (CLSI) guidelines[71]. Briefly, the bacteria were grown on Mueller-Hinton (MH), TSA or BHI

agar plates with disks containing various compounds. Initially the bacteria were streaked out on LB, TSA or BHI agar plates. The next morning a few colonies were suspended in saline to reach a final OD_{600} of 0.2. Suspensions of cells were evenly distributed on dry MH agar plates with a cotton swap. Paper disks containing either 0.16, 0.8, 4, 20, 100 or 500 µg of the respective compounds were placed on the agar plates. Vancomycin (30 µg/disk) and Ampicillin (10 µg/disk) were used as controls. After 20 h the antimicrobial activity of the compounds were evaluated. We considered a compound as antimicrobial if it showed a clear zone of growth inhibition comparable to the control.

4.3.7 Determination of the minimal inhibitory concentration (MIC) and minimal bactericidal concentration (BAC)

The minimal inhibitory concentration (MIC) of the tested compounds was determined by the two-fold serial broth (LB, BHI or THB Broth medium) dilution method in 96 well plates (Fisher Scientific Co.) according to CLSI guidelines[72]. Briefly, each well contained a cell density of 3-7 x 10^5 cfu/ml; compound concentrations ranging from 0.5 to 128 µg/ml. After incubation for 20 hours at 37 °C MIC`s were read as the lowest concentration of the compound that completely inhibited growth. Additional the minimal bactericidal concentration (MBC) that kills > 99.99 % of the starting inoculum was determined. 10 µl of the wells that did not support growth were spotted on agar plates. MBC`s were read the following day as spots with less than 5 colonies.

To test adjuvants effect on the bacterial resistance, a panel of clinical bacterial strains having different resistance mechanisms was selected. Five resistant isolates were tested: three *Echerichia coli* isolates: G28 (with betalactamase, amoxicillin resistant), G02 (ofloxacin-resistant), ARS 108 (with extended spectrum betalactamase (ESBL), third cephalosporins generation resistant) and two *Staphylococcus aureus*: C1P15 (with penicillinase, penicillin G resistant) and C1BP13 (meticillin-resistant (MRSA)). Two strains of *S. aureus* (ATCC 29213)

and *E. coli* (ATCC 25922) have been used as quality control. MICs and MBCs of a panel of antibiotics including β-lactams (amoxicillin (AMX), cloxacillin (CLX), penicillin G (PNG), cefotaxime (CTX)) and quinolone (ofloxacin (OFX)), were determined by the broth microdilution method as described by EUCAST (European Commitee of Antimicrobial Susceptibility Testing). The bacterial inoculum was set at 10^6 bacteria per mL. Tests were carried out in triplicate with or without fixed concentration (25 µg/mL) of adjuvants. To determine the MBC, the dilution representing the MIC and at least two of the more concentrated test product dilutions are plated and enumerated to determine viable CFU (Coloning Forming Unit)/mL. In parallel, the effect of all adjuvants used without antibiotic was tested on the resistant isolates with growing concentrations of adjuvants.

4.3.8 Determination of bactericidal and or bacteriostatic activity of compounds 6d and 6e

Growth curves with *B. subtilis* JH642 were performed to distinguish whether compounds **6d** and **6e** are bactericidal or bacteriostatic. *B. subtilis* was grown in 5 ml LB overnight. The following morning 20 ml LB was inoculated to a starting OD_{600} of 0.05. As soon as the culture reached an OD_{600} of 0.5 to 0.6 the additives were added to the culture. The antibiotics chloramphenicol and vancomycin served as control. Growth of the cultures was routinely measured before and after addition of the substances for several hours. Similar assays were also performed for *S. aureus*, however for handling purposes with fewer time points and in smaller volume.

4.3.9 Hemolysis assay

Hemolytic activity of the thiophen derivatives was determined as previously described[73]. Briefly, Sheep red blood cells (RBCs) were washed 3 times with phosphate buffered saline. Each hemeolysis reaction contained 2% (v/v) RBC, 10% DMSO and 1 mM of the respective compounds. Samples were incubated for 45 min at 37 °C under agitation at 100 rpm. Controls contained either no compounds or H_2O (100% lysis of RBCs). After incubation the RBCs

were separated from the remaining reaction mixture by centrifugation at 900 x g and 4 C°. Hemolytic activities of the compounds or lack thereof were determined visually.

ASSOCIATED CONTENT

Supporting information

The supporting information is available free of charge on the ACS Publications website at DOI.

The HRMS, HPLC, ^{1}H NMR, ^{13}CNMR, ^{135}DEPT NMR spectra for some important compounds (pdf). The molecular formula strings (CSV).

Accession codes

No accession codes were deposited.

AUTHOR INFORMATIONS

Corresponding author

*E-mail: zohra.benfodda@unimes.fr. Phone+33 04 66 27 95 89.

*E-mail: Szurmant@scripps.edu. Phone+1 858 784 7945.

#These authors contributed equally to this work.

ΨThese authors jointly supervised this work.

Notes

The authors declare no competing financial interest.

Author contributions

Z.B., P.M., H.S, C.D.R, AL wrote the manuscript. A.L. designed the compounds, T.B. synthesized the compounds, C.Z. performed the biological experiment, J.P.L and C.D.R. designed the adjuvant experiments. All authors have given approval to the final version of the manuscript.

ABBREVIATIONS USED

Asp, aspartic acid; Asn, Asparagine; ATP, adenosine triphosphate; *B. subtilis*, *Bacillus subtilis*; BHI, brain heart infusion; CLSI, clinical and laboratory standards institute; 13C NMR, carbon nuclear magnetic resonance; CA, catalytic ATP-binding domain; DNA, deoxyribonucleic acid; DMF, N,N-dimethylformamide; DMSO, dimethylsulfoxyde; EDTA, ethylenediaminetetraacetic acid; *E. coli, Escherichia coli*; *E. faecalis, Enterococcus faecalis;* EtOAc, ethylacetate; ESBL, Extended spectrum beta lactamase; 1H NMR, proton nuclear magnetic resonance; HK, histidine kinase; HRMS, High resolution mass spectra; IR, infrared; IC50, half-maximal inhibitory concentration; HPLC, high performance liquid chromatography; IreK, intrinsic resistance of enterococci kinase; Ile, Isoleucine; MS, mass spectroscopy; MeOH, Methanol; MBC, minimum bactericidal concentration; MIC, minimum inhibitory concentration; MRSA, *methicillin-resistant Staphylococcus aureus*; PCR, polymerase chain reaction; PE, petroleum ether; PDB, protein data base; RR, response regulator; SDS-PAGE, sodium dodecyl sulfate poly acrylamide gel electrophoresis; Tof, time of flight; TSA, tryptic soy agar; Tyr, tyrosine; TCSs, two-component signal transduction systems; UPLC, ultra-performance liquid chromatography.

ACKNOWLEDGMENTS

H.S. was supported by grant no. GM106085 from the U.S. National Institute of General Medical Sciences, National Institutes of Health. The authors thank Marta Perego, Christopher Kristich and Liang Tang for the purified recombinant proteins and expression plasmids. D.B., T.B., Z.B., P.M. and A.L. thank the French "ministère de l'éducation nationale, de l'enseignement supérieur et de la recherche" and the University of Nîmes for their financial support.

REFERENCES

(1) Kumarasamy, K. K.; Toleman, M. A.; Walsh, T. R.; Bagaria, J.; Butt, F.; Balakrishnan, R.; Chaudhary, U.; Doumith, M.; Giske, C. G.; Irfan, S.; Krishnan, P.; Kumar, A. V.; Maharjan, S.; Mushtaq, S.; Noorie, T.; Paterson, D. L.; Pearson, A.; Perry, C.; Pike, R.; Rao, B.; Ray, U.; Sarma, J. B.; Sharma, M.; Sheridan, E.; Thirunarayan, M. A.; Turton, J.; Upadhyay, S.; Warner, M.; Welfare, W.; Livermore, D. M.; Woodford, N. Emergence of a New Antibiotic Resistance Mechanism in India, Pakistan, and the UK: A Molecular, Biological, and Epidemiological Study. *Lancet Infect. Dis.* **2010**, *10* (9), 597–602.

(2) Deurenberg, R. H.; Stobberingh, E. E. The Molecular Evolution of Hospital- and Community-Associated Methicillin-Resistant Staphylococcus Aureus. *Curr. Mol. Med.* **2009**, *9* (2), 100–115.

(3) de Kraker, M. E. A.; Wolkewitz, M.; Davey, P. G.; Koller, W.; Berger, J.; Nagler, J.; Icket, C.; Kalenic, S.; Horvatic, J.; Seifert, H.; Kaasch, A. J.; Paniara, O.; Argyropoulou, A.; Bompola, M.; Smyth, E.; Skally, M.; Raglio, A.; Dumpis, U.; Kelmere, A. M.; Borg, M.; Xuereb, D.; Ghita, M. C.; Noble, M.; Kolman, J.; Grabljevec, S.; Turner, D.; Lansbury, L.; Grundmann, H.; BURDEN Study Group. Clinical Impact of Antimicrobial Resistance in European Hospitals: Excess Mortality and Length of Hospital Stay Related to Methicillin-Resistant Staphylococcus Aureus Bloodstream Infections. *Antimicrob. Agents Chemother.* **2011**, *55* (4), 1598–1605.

(4) Walsh, C. Molecular Mechanisms That Confer Antibacterial Drug Resistance. *Nature* **2000**, *406* (6797), 775–781.

(5) Levings, R. S.; Lightfoot, D.; Partridge, S. R.; Hall, R. M.; Djordjevic, S. P. The Genomic Island SGI1, Containing the Multiple Antibiotic Resistance Region of Salmonella Enterica Serovar Typhimurium DT104 or Variants of It, Is Widely Distributed in Other S. Enterica Serovars. *J. Bacteriol.* **2005**, *187* (13), 4401–4409.

(6) Schnellmann, C.; Gerber, V.; Rossano, A.; Jaquier, V.; Panchaud, Y.; Doherr, M. G.; Thomann, A.; Straub, R.; Perreten, V. Presence of New mecA and mph(C) Variants Conferring Antibiotic Resistance in Staphylococcus Spp. Isolated from the Skin of Horses before and after Clinic Admission. *J. Clin. Microbiol.* **2006**, *44* (12), 4444–4454.

(7) Elshaarawy, R. F. M.; Janiak, C. Toward New Classes of Potent Antibiotics: Synthesis and Antimicrobial Activity of Novel Metallosaldach–imidazolium Salts. *Eur. J. Med. Chem.* **2014**, *75*, 31–42.

(8) Govan, J. R.; Deretic, V. Microbial Pathogenesis in Cystic Fibrosis: Mucoid

Pseudomonas Aeruginosa and Burkholderia Cepacia. *Microbiol. Rev.* **1996**, *60* (3), 539–574.

(9) Norrby, S. R.; Nord, C. E.; Finch, R. Lack of Development of New Antimicrobial Drugs: A Potential Serious Threat to Public Health. *Lancet Infect. Dis.* **2005**, *5* (2), 115–119.

(10) O'Driscoll, C. $100 Trillion Resistance Cost. *Chem. Ind.* **2015**, *79* (1), 11.

(11) Fernebro, J. Fighting Bacterial infections—Future Treatment Options. *Drug Resist. Updat.* **2011**, *14* (2), 125–139.

(12) Jabes, D. The Antibiotic R&D Pipeline: An Update. *Antimicrobials/Genomics* **2011**, *14* (5), 564–569.

(13) Stanton, T. B. A Call for Antibiotic Alternatives Research. *Trends Microbiol.* **2013**, *21* (3), 111–113.

(14) Wang, S. Bacterial Two-Component Systems: Structures and Signaling Mechanisms. In *Protein Phosphorylation in Human Health*; Huang, C., Ed.; InTech, 2012.

(15) Thomason, P.; Kay, R. Eukaryotic Signal Transduction via Histidine-Aspartate Phosphorelay. *J. Cell Sci.* **2000**, *113* (18), 3141–3150.

(16) Martin, P. K.; Li, T.; Sun, D.; Biek, D. P.; Schmid, M. B. Role in Cell Permeability of an Essential Two-Component System in Staphylococcus Aureus. *J. Bacteriol.* **1999**, *181* (12), 3666–3673.

(17) Watanabe, T.; Hashimoto, Y.; Yamamoto, K.; Hirao, K.; Ishihama, A.; Hino, M.; Utsumi, R. Isolation and Characterization of Inhibitors of the Essential Histidine Kinase, YycG in Bacillus Subtilis and Staphylococcus Aureus. *J. Antibiot. (Tokyo)* **2003**, *56* (12), 1045–1052.

(18) Fabret, C.; Hoch, J. A. A Two-Component Signal Transduction System Essential for Growth of Bacillus Subtilis: Implications for Anti-Infective Therapy. *J. Bacteriol.* **1998**, *180* (23), 6375–6383.

(19) Hancock, L.; Perego, M. Two-Component Signal Transduction in Enterococcus Faecalis. *J. Bacteriol.* **2002**, *184* (21), 5819–5825.

(20) Barrett, J. F.; Hoch, J. A. Two-Component Signal Transduction as a Target for Microbial Anti-Infective Therapy. *Antimicrob. Agents Chemother.* **1998**, *42* (7), 1529–1536.

(21) Macielag, M. J.; Goldschmidt, R. Inhibitors of Bacterial Two-Component Signalling Systems. *Expert Opin. Investig. Drugs* **2000**, *9* (10), 2351–2369.

(22) Matsushita, M.; Janda, K. D. Histidine Kinases as Targets for New Antimicrobial Agents. *Bioorg. Med. Chem.* **2002**, *10* (4), 855–867.

(23) Stock, A. M.; Robinson, V. L.; Goudreau, P. N. Two-Component Signal Transduction. *Annu. Rev. Biochem.* **2000**, *69*, 183–215.

(24) Gooderham, W. J.; Hancock, R. E. W. Regulation of Virulence and Antibiotic Resistance by Two-Component Regulatory Systems in Pseudomonas Aeruginosa. *FEMS Microbiol. Rev.* **2009**, *33* (2), 279–294.

(25) García-Calderón, C. B.; Casadesús, J.; Ramos-Morales, F. Rcs and PhoPQ Regulatory Overlap in the Control of Salmonella Enterica Virulence. *J. Bacteriol.* **2007**, *189* (18), 6635–6644.

(26) Xue, T.; You, Y.; Hong, D.; Sun, H.; Sun, B. The Staphylococcus Aureus KdpDE Two-Component System Couples Extracellular K+ Sensing and Agr Signaling to Infection Programming . *Infect. Immun.* **2011**, *79* (6), 2154–2167.

(27) Gotoh, Y.; Eguchi, Y.; Watanabe, T.; Okamoto, S.; Doi, A.; Utsumi, R. Two-Component Signal Transduction as Potential Drug Targets in Pathogenic Bacteria. *Curr. Opin. Microbiol.* **2010**, *13* (2), 232–239.

(28) Stephenson, K.; Hoch, J. A. Virulence- and Antibiotic Resistance-Associated Two-Component Signal Transduction Systems of Gram-Positive Pathogenic Bacteria as Targets for Antimicrobial Therapy. *Pharmacol. Ther.* **2002**, *93* (2–3), 293–305.

(29) Bem, A. E.; Velikova, N.; Pellicer, M. T.; Baarlen, P. van; Marina, A.; Wells, J. M. Bacterial Histidine Kinases as Novel Antibacterial Drug Targets. *ACS Chem. Biol.* **2015**, *10* (1), 213–224.

(30) Worthington, R. J.; Blackledge, M. S.; Melander, C. Small-Molecule Inhibition of Bacterial Two-Component Systems to Combat Antibiotic Resistance and Virulence. *Future Med. Chem.* **2013**, *5* (11), 1265–1284.

(31) Casino, P.; Rubio, V.; Marina, A. The Mechanism of Signal Transduction by Two-Component Systems. *Curr. Opin. Struct. Biol.* **2010**, *20* (6), 763–771.

(32) Stephenson, K.; Yamaguchi, Y.; Hoch, J. A. The Mechanism of Action of Inhibitors of Bacterial Two-Component Signal Transduction Systems. *J. Biol. Chem.* **2000**, *275* (49), 38900–38904.

(33) Gilmour, R.; Foster, J. E.; Sheng, Q.; McClain, J. R.; Riley, A.; Sun, P.-M.; Ng, W.-L.; Yan, D.; Nicas, T. I.; Henry, K.; Winkler, M. E. New Class of Competitive Inhibitor of Bacterial Histidine Kinases. *J. Bacteriol.* **2005**, *187* (23), 8196–8200.

(34) Gao, R.; Stock, A. M. Biological Insights from Structures of Two-Component Proteins. *Annu. Rev. Microbiol.* **2009**, *63*, 133–154.

(35) Škedelj, V.; Tomašić, T.; Mašič, L. P.; Zega, A. ATP-Binding Site of Bacterial Enzymes as a Target for Antibacterial Drug Design. *J. Med. Chem.* **2011**, *54* (4), 915–929.

(36) Schreiber, M.; Res, I.; Matter, A. Protein Kinases as Antibacterial Targets. *Curr. Opin.*

Cell Biol. **2009**, *21* (2), 325–330.

(37) Hilliard, J. J.; Goldschmidt, R. M.; Licata, L.; Baum, E. Z.; Bush, K. Multiple Mechanisms of Action for Inhibitors of Histidine Protein Kinases from Bacterial Two-Component Systems. *Antimicrob. Agents Chemother.* **1999**, *43* (7), 1693–1699.

(38) Qin, Z.; Zhang, J.; Xu, B.; Chen, L.; Wu, Y.; Yang, X.; Shen, X.; Molin, S.; Danchin, A.; Jiang, H.; Qu, D. Structure-Based Discovery of Inhibitors of the YycG Histidine Kinase: New Chemical Leads to Combat Staphylococcus Epidermidis Infections. *BMC Microbiol.* **2006**, *6*, 96.

(39) Fakhruzzaman, M.; Inukai, Y.; Yanagida, Y.; Kino, H.; Igarashi, M.; Eguchi, Y.; Utsumi, R. Study on in Vivo Effects of Bacterial Histidine Kinase Inhibitor, Waldiomycin, in Bacillus Subtilis and Staphylococcus Aureus. *J. Gen. Appl. Microbiol.* **2015**, *61* (5), 177–184.

(40) Velikova, N.; Fulle, S.; Manso, A. S.; Mechkarska, M.; Finn, P.; Conlon, J. M.; Oggioni, M. R.; Wells, J. M.; Marina, A. Putative Histidine Kinase Inhibitors with Antibacterial Effect against Multi-Drug Resistant Clinical Isolates Identified by in Vitro and in Silico Screens. *Sci. Rep.* **2016**, *6*, 26085.

(41) van Rensburg, J. J.; Fortney, K. R.; Chen, L.; Krieger, A. J.; Lima, B. P.; Wolfe, A. J.; Katz, B. P.; Zhang, Z.-Y.; Spinola, S. M. Development and Validation of a High-Throughput Cell-Based Screen to Identify Activators of a Bacterial Two-Component Signal Transduction System. *Antimicrob. Agents Chemother.* **2015**, *59* (7), 3789–3799.

(42) Wilke, K. E.; Francis, S.; Carlson, E. E. Inactivation of Multiple Bacterial Histidine Kinases by Targeting the ATP-Binding Domain. *ACS Chem. Biol.* **2015**, *10* (1), 328–335.

(43) Tanaka, T.; Saha, S. K.; Tomomori, C.; Ishima, R.; Liu, D.; Tong, K. I.; Park, H.; Dutta, R.; Qin, L.; Swindells, M. B.; Yamazaki, T.; Ono#, A. M.; Kainosho#, M.; Inouye, M.; Ikura, M. NMR Structure of the Histidine Kinase Domain of the E. Coli Osmosensor EnvZ. *Nature* **1998**, *396* (6706), 88–92.

(44) Dutta, R.; Inouye, M. GHKL, an Emergent ATPase/kinase Superfamily. *Trends Biochem. Sci.* **2000**, *25* (1), 24–28.

(45) Guarnieri, M. T.; Zhang, L.; Shen, J.; Zhao, R. The Hsp90 Inhibitor Radicicol Interacts with the ATP-Binding Pocket of Bacterial Sensor Kinase PhoQ. *J. Mol. Biol.* **2008**, *379* (1), 82–93.

(46) Celikel, R.; Veldore, V. H.; Mathews, I.; Devine, K. M.; Varughese, K. I. ATP Forms a Stable Complex with the Essential Histidine Kinase WalK (YycG) Domain. *Acta Crystallogr. Sect. D* **2012**, *68* (7), 839–845.

(47) Corbett, K. D.; Berger, J. M. Structural Basis for Topoisomerase VI Inhibition by the

Anti-Hsp90 Drug Radicicol. *Nucleic Acids Res.* **2006**, *34* (15), 4269–4277.

(48) Brvar, M.; Perdih, A.; Renko, M.; Anderluh, G.; Turk, D.; Solmajer, T. Structure-Based Discovery of Substituted 4,5′-Bithiazoles as Novel DNA Gyrase Inhibitors. *J. Med. Chem.* **2012**, *55* (14), 6413–6426.

(49) Sherer, B. A.; Hull, K.; Green, O.; Basarab, G.; Hauck, S.; Hill, P.; Loch III, J. T.; Mullen, G.; Bist, S.; Bryant, J.; Boriack-Sjodin, A.; Read, J.; DeGrace, N.; Uria-Nickelsen, M.; Illingworth, R. N.; Eakin, A. E. Pyrrolamide DNA Gyrase Inhibitors: Optimization of Antibacterial Activity and Efficacy. *Bioorg. Med. Chem. Lett.* **2011**, *21* (24), 7416–7420.

(50) Grillot, A.-L.; Tiran, A. L.; Shannon, D.; Krueger, E.; Liao, Y.; O'Dowd, H.; Tang, Q.; Ronkin, S.; Wang, T.; Waal, N.; Li, P.; Lauffer, D.; Sizensky, E.; Tanoury, J.; Perola, E.; Grossman, T. H.; Doyle, T.; Hanzelka, B.; Jones, S.; Dixit, V.; Ewing, N.; Liao, S.; Boucher, B.; Jacobs, M.; Bennani, Y.; Charifson, P. S. Second-Generation Antibacterial Benzimidazole Ureas: Discovery of a Preclinical Candidate with Reduced Metabolic Liability. *J. Med. Chem.* **2014**, *57* (21), 8792–8816.

(51) Martin, L.; Catherinot, V.; Labesse, G. kinDOCK: A Tool for Comparative Docking of Protein Kinase Ligands. *Nucleic Acids Res.* **2006**, *34* (suppl 2), W325–W329.

(52) Pons, J.-L.; Labesse, G. @TOME-2: A New Pipeline for Comparative Modeling of Protein–ligand Complexes. *Nucleic Acids Res.* **2009**, *37* (suppl 2), W485–W491.

(53) Catherinot, V.; Labesse, G. ViTO: Tool for Refinement of Protein Sequence–structure Alignments. *Bioinformatics* **2004**, *20* (18), 3694–3696.

(54) Neudert, G.; Klebe, G. DSX: A Knowledge-Based Scoring Function for the Assessment of Protein–Ligand Complexes. *J. Chem. Inf. Model.* **2011**, *51* (10), 2731–2745.

(55) Korb, O.; Stützle, T.; Exner, T. E. Empirical Scoring Functions for Advanced Protein−Ligand Docking with PLANTS. *J. Chem. Inf. Model.* **2009**, *49* (1), 84–96.

(56) ten Brink, T.; Exner, T. E. Influence of Protonation, Tautomeric, and Stereoisomeric States on Protein−Ligand Docking Results. *J. Chem. Inf. Model.* **2009**, *49* (6), 1535–1546.

(57) Brink, T. ten; Exner, T. E. pKa Based Protonation States and Microspecies for Protein–ligand Docking. *J. Comput. Aided Mol. Des.* **2010**, *24* (11), 935–942.

(58) Miyaura, N.; Suzuki, A. Palladium-Catalyzed Cross-Coupling Reactions of Organoboron Compounds. *Chem. Rev.* **1995**, *95* (7), 2457–2483.

(59) Lucas, B. Heterocyclic Compounds and Their Use as Inhibitors of Pi3k Activity. WO2012003262 (A1), January 5, 2012.

(60) Carbonne, A.; Arnaud, I.; Maugat, S.; Marty, N.; Dumartin, C.; Bertrand, X.; Bajolet, O.; Savey, A.; Fosse, T.; Eveillard, M.; Sénéchal, H.; Coignard, B.; Astagneau, P.; Jarlier, V.;

(BMR-Raisin), on behalf of the M. S. N. S. G. National Multidrug-Resistant Bacteria (MDRB) Surveillance in France through the RAISIN Network: A 9 Year Experience. *J. Antimicrob. Chemother.* **2013**, *68* (4), 954–959.

(61) Tentolouris, N.; Petrikkos, G.; Vallianou, N.; Zachos, C.; Daikos, G. L.; Tsapogas, P.; Markou, G.; Katsilambros, N. Prevalence of Methicillin-Resistant Staphylococcus Aureus in Infected and Uninfected Diabetic Foot Ulcers. *Clin. Microbiol. Infect.* **2006**, *12* (2), 186–189.

(62) O'Boyle, N. M.; Banck, M.; James, C. A.; Morley, C.; Vandermeersch, T.; Hutchison, G. R. Open Babel: An Open Chemical Toolbox. *J. Cheminformatics* **2011**, *3*, 33.

(63) Conde, S.; Corral, C.; Lissavetzky, J. E- and Z-Isomerism of 2-Acetylthiophene Oximes. *J. Heterocycl. Chem.* **1985**, *22* (2), 301–304.

(64) Slevin, Å.; Koolmeister, T.; Scobie, M. A Versatile Synthesis of Diverse 3,4-Fused Cinnolines via the Base-Catalysed Condensation of 2-Amino-2′-Nitrobiaryls. *Chem. Commun.* **2007**, No. 24, 2506–2508.

(65) Bugge, S.; Kaspersen, S. J.; Larsen, S.; Nonstad, U.; Bjørkøy, G.; Sundby, E.; Hoff, B. H. Structure–activity Study Leading to Identification of a Highly Active Thienopyrimidine Based EGFR Inhibitor. *Eur. J. Med. Chem.* **2014**, *75*, 354–374.

(66) Valant, C.; May, L. T.; Aurelio, L.; Chuo, C. H.; White, P. J.; Baltos, J.-A.; Sexton, P. M.; Scammells, P. J.; Christopoulos, A. Separation of on-Target Efficacy from Adverse Effects through Rational Design of a Bitopic Adenosine Receptor Agonist. *Proc. Natl. Acad. Sci.* **2014**, *111* (12), 4614–4619.

(67) Ashwell, S.; Gero, T.; Ioannidis, S.; Janetka, J.; Lyne, P.; Su, M.; Toader, D.; Yu, D.; Yu, Y. Thiophene Derivatives as Chk 1 Inihibitors. WO2005066163 (A2), July 21, 2005.

(68) Prasad, B. A. B.; Gilbertson, S. R. One-Pot Synthesis of Unsymmetrical N-Heterocyclic Carbene Ligands from N-(2-Iodoethyl)arylamine Salts. *Org. Lett.* **2009**, *11* (16), 3710–3713.

(69) Kristich, C. J.; Little, J. L.; Hall, C. L.; Hoff, J. S. Reciprocal Regulation of Cephalosporin Resistance in Enterococcus Faecalis. *mBio* **2011**, *2* (6), e00199-111.

(70) Igarashi, M.; Watanabe, T.; Hashida, T.; Umekita, M.; Hatano, M.; Yanagida, Y.; Kino, H.; Kimura, T.; Kinoshita, N.; Inoue, K.; Sawa, R.; Nishimura, Y.; Utsumi, R.; Nomoto, A. Waldiomycin, a Novel WalK-Histidine Kinase Inhibitor from Streptomyces Sp. MK844-mF10. *J. Antibiot. (Tokyo)* **2013**, *66* (8), 459–464.

(71) Wayne, P. Performance Standards for Antimicrobial Disk Susceptibility Tests; Approved Standards-9th Ed. *Clinical and Laboratory Standards Institute.* 2006, p CLSI document M2-A9.

(72) Wayne, P. Methods for Dilution Antimicrobial Susceptibility Tests for Bacteria That Grow Aerobically; Approved Standards-9th Ed. *Clinical and Laboratory Standards Institute.* 2012, p CLSI document M07-A9.

(73) Kent, K. A.; Lemcke, R. M.; Lysons, R. J. Production, Purification and Molecular Weight Determination of the Haemolysin of Treponema Hyodysenteriae. *J. Med. Microbiol.* **1988**, *27* (3), 215–224.

Figure 1. The two-component system signaling (TCS) cascade. A phosphoryl group is transferred from the Catalytic domain (CA) to a conserved His-residue of the HK and from there at a conserved sp-residue of response regulator (RR). A typical function for the RR is gene regulation.

Figure 2. A: X-ray crystal structure of the ATP-binding domain of WalK (PDB: 3SL2). **B**: Binding mode of ATP with ATP-lid loop.

Figure 3. Superposition of Histidine kinase in green with ATP in pink and Gyrase B in blue with its pyrrolamide inhibitor in gold. **B**: Evaluation of the HK pyrrolamide complex with DSX. Blue spheres represents favorable interactions where as red spheres represents bad interactions. Blue lines represent favorable distances whereas red lines represent bad distances. **C**: Zoom of the pyrrolamide ligand inside the Histidine domain of WalK. **D:** Pyrrolamide inhibitor.

Figure 4. Design Strategy.

Figure 5. Chemical library designed.

Figure 6. A: Binding pose of compound **6a** into the ATP-binding site of WalK. **B:** Evaluation of compound **6a** docked into ATP-Binding site using PLANTS with DSX. Blue spheres represent favorable interactions whereas red spheres represents bad interactions. Blue lines represent favorable distances whereas red lines represent bad distances.

Figure 7. A screen with cytoplasmic WalK fragments identifies eight compounds with kinase inhibitory activity.

Two *Bacillus subtilis* cytoplasmic histidine kinases constructs, $WalK^{272-612}$ and $WalK^{204-612}$, were subjected to autophosphorylation in the presence of 1 mMγ-^{32}P-labeled ATP and in the presence or absence (control) of 1 mM of putative kinase inhibitors. Autophosphorylation of WalK kinase was terminated after 3 minutes by addition of SDS-sample buffer and the reactions were subjected to SDS-PAGE followed by phosphor-imaging. Bands on the gel indicate the extent of the autophosphorylation reaction. Compounds, whose presence caused visual reduction in autophosphorylation activity are indicated by an arrow and were selected for further analysis**. (A)** Compounds used were **6g**, **6h**, **6b**, **7a**, **6c**, **6a**, **6j**, and **6k**; top panel $WalK^{204-612}$; bottom panel $WalK^{272-612}$. **(B)** Compounds used were **6t**, **6s**, **6d**, **6e**, **6f**, **6m**, **6o**, and **6u**; top panel $WalK^{204-612}$; bottom Panel $WalK^{272-612}$. **(C)** Compounds used were **7c**, **6i**, **6l**, **6n**, **7b**, **6p**, **6q**, and **6r**; top panel $WalK^{204-612}$; bottom panel $WalK^{272-612}$.

Figure 8. Compound **6e** inhibits autophosphorylation of histidine kinases PhoR, ResE and WalK but not serine/threonine kinase IreK or DNA-gyrase.

Autophosphorylation of kinases and DNA gyrase-catalyzed supercoiling were performed as described in materials and methods. In contrast to Figure 1, protein concentrations, ATP concentrations and time points were adjusted for IC_{50} determination. **(A)** Autophosphorylation activity of cytoplasmic constructs of PhoR (top panel), ResE (middle panel) and WalK (bottom panel) in the presence of increasing amounts of compound **6e** (0; 6.25; 12.5; 25; 50; 100; 200; 400; 800 μM). The autophosphorylation activity was monitored after 60, 8 and 40 min respectively. These time points were chosen imperially to reflect a linear rate of autophosphorylation for each kinase. **(B)** The serine/threonine kinase IreK from *E. faecalis* was subjected to autophosphorylation in analogy to the assays performed for histidine kinases with increasing amounts of compound **6e** (0; 6.25; 12.5; 25; 50; 100; 200; 400; and 800 μM). The autophosphorylation activity was monitored after 15 min. **(C)** *E. coli* DNA gyrase-catalyzed supercoiling in the presence and absence of indicated concentrations of compound **6e** was monitored. Ciprofloxacin (200 nM) was used as a positive control for gyrase inhibition. Each reaction contained 1U gyrase and 75ng gyrase substrate according to manufacturer recommendation.

Figure 9. The histidine kinase inhibitors **6d** and **6e** exhibit antimicrobial activity (A, B).

The Kirby-Bauer disk diffusion susceptibility assay was used to determine the antimicrobial activity of the selected compounds (see material and methods). **(A)** Antimicrobial activity screen of the eight selected compounds against methicillin resistant *S. aureus* (MRSA). A disk containing 30μg vancomycin was used as control (c). 100μg of compounds **6h** (1), **6c** (2), **6k** (3), **6s** (4), **6d** (5), **6e** (6), **7c** (7) and **6i** (8) was applied to each disk. **(B)** Dose-dependent antimicrobial activities of the compounds **6d** and **6e** against MRSA. 30μg vancomycin was used as control (c). Decreasing amounts of **6d** (left) and **6e** (right). [1 and 7 = 500 μg; 2 and 8 = 100 μg; 3 and 9 = 20 μg; 4 and 10 = 4 μg; 5 and 11 = 0.8 μg ; 6 and 12 = 0.16 μg] **(C)** Effect of compounds **6d** and **6e** on exponentially growing *B. subtilis* cultures was monitored. To determine whether compounds **6d** and **6e** exhibit bactericidal or bacteriostatic activity *B. subtilis* JH642 was grown in LB medium at 37 °C. Vancomycin (Va) and chloramphenicol (Cm) served as controls. Optical density (OD) at a wavelength of 600 nm was routinely measured. At an OD_{600} of 0.5-0.6 (indicated by an arrow) 50μg compounds **6d** (squares), **6e** (triangles facing up), chloramphenicol (triangles facing down) or vancomycin (diamonds) was added. *B. subtilis* JH642 was also grown without additives (circles).

Scheme 1. Synthesis of Thiophene derivatives **6a-u**[a].

Scheme 2. Synthesis of acetamide **3**[a].

Scheme 3. Synthesis of Thiophene derivatives **7a-c**[a].

Scheme 4. Synthesis of amine hydrochloride salts **8a-i**[a].

Table1. DSX score of docked compounds.

Table 2. Chemical structure, chemical data and purity of synthesized compounds.

Table 3. Conditions of Suzuki coupling to obtain Thiophene derivatives **6a-u** and **7a-c**.

Table 4. IC_{50} values against histidine kinases PhoR, ResE and WalK, Ser/Thr kinase IreK and DNA-gyrase for selected compounds.

Table 5. Antibacterial activity of compounds **6d** and **6e** against reference Gram-positive and Gram-negative bacteria. Minimal inhibitory concentration (MIC) and minimal bactericidal concentration (MBC) are in μg/ml.

Table 6. Antibiotic susceptibility of four *Escherichia coli* isolates and three *Staphylococcus aureus* isolates with and without histidine kinase inhibitor **6d**.

Figure 1. The two-component system signaling (TCS) cascade. A phosphoryl group is transferred from the Catalytic domain (CA) to a conserved His-residue of the HK and from there at a conserved sp-residue of response regulator (RR). A typical function for the RR is gene regulation.

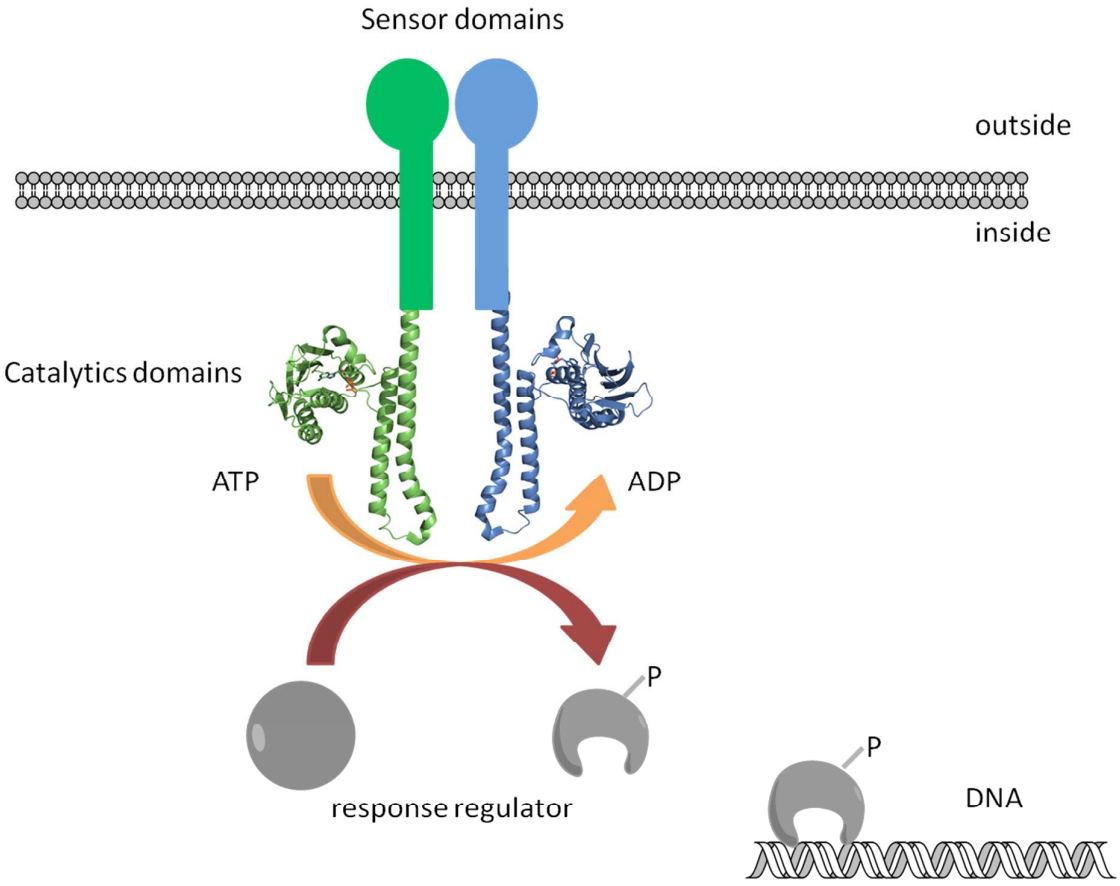
Sensor domains
outside
inside
Catalytics domains
ATP
ADP
P
response regulator
P
DNA

Figure 2. A: X-ray crystal structure of the ATP-binding domain of WalK (PDB: 3SL2). **B**: Binding mode of ATP with ATP-lid loop.

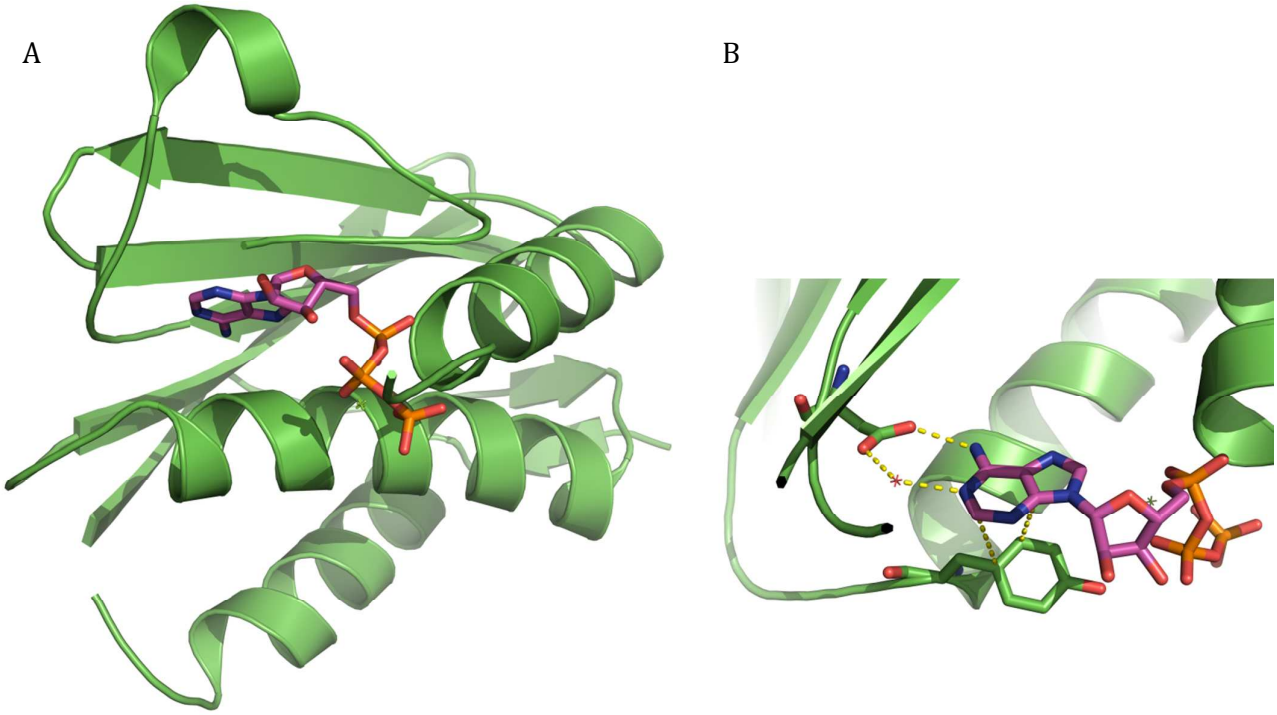

Figure 3. Superposition of Histidine kinase in green with ATP in pink and Gyrase B in blue with its pyrrolamide inhibitor in gold. **B**: Evaluation of the HK pyrrolamide complex with DSX. Blue spheres represents favorable interactions where as red spheres represents bad interactions. Blue lines represent favorable distances whereas red lines represent bad distances. **C**: Zoom of the pyrrolamide ligand inside the Histidine domain of WalK. **D:** Pyrrolamide inhibitor.

A

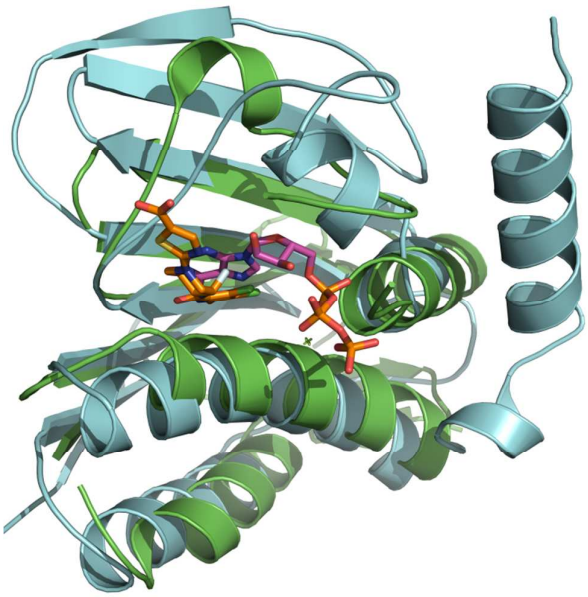

B

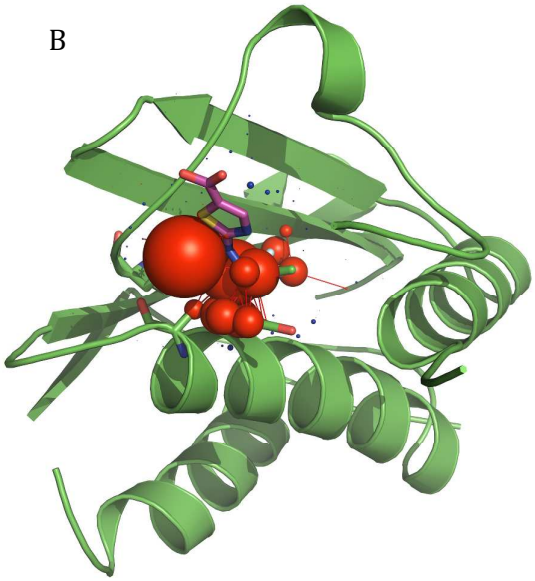

C

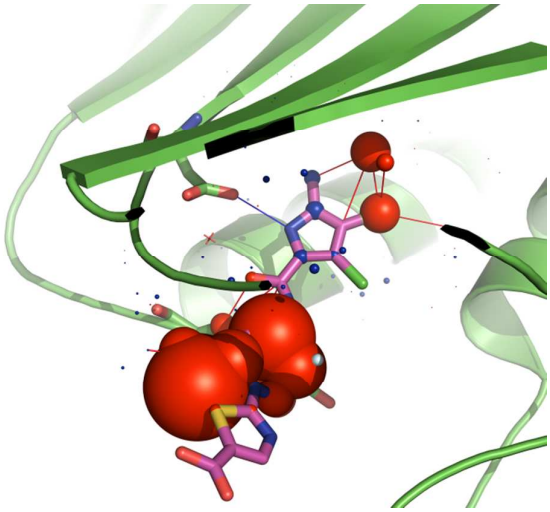

D

Pyrrolamide inhibitor

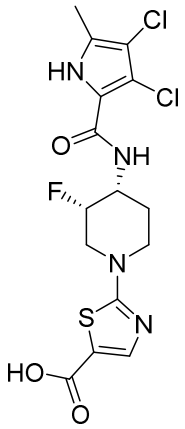

Figure 4. Design Strategy

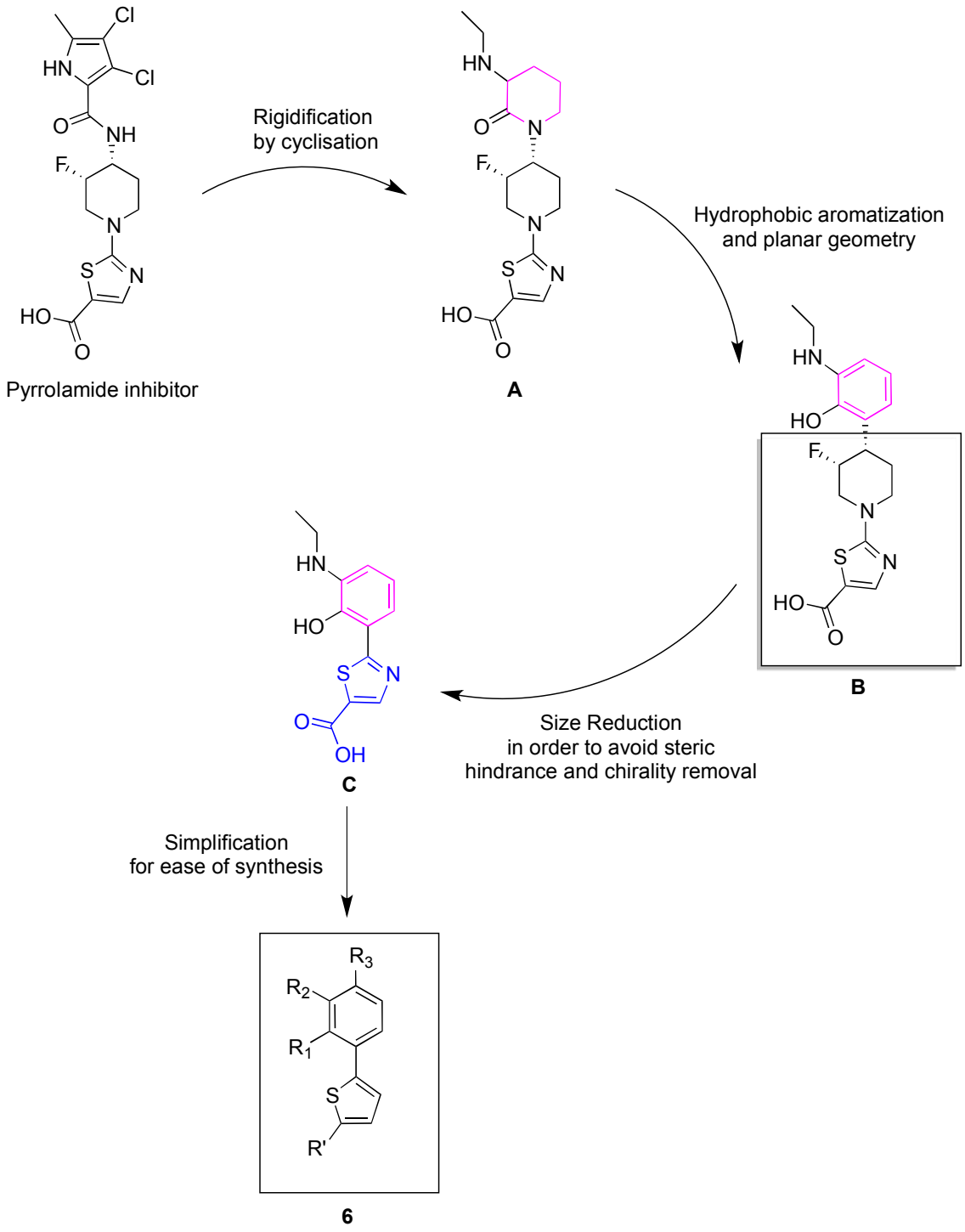

Figure 5. Chemical library designed.

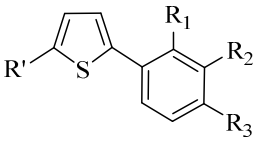

6a: R'=NO_2, R_1=NH_2, R_2=H, R_3= H
6b: R'=NO_2, R_1= H, R_2=NH_2, R_3= H
6c: R'=NO_2, R_1= H, R_2=H, R_3= NH_2
6d: R'=NO_2, R_1=OH, R_2=H, R_3= H
6e: R'=NO_2, R_1= H, R_2=OH, R_3= H
6f: R'=NO_2, R_1= H, R_2=H, R_3= OH
6g: R'=CH_3CO, R_1=NH_2, R_2=H, R_3= H
6h: R'=CH_3CO, R_1= H, R_2=NH_2, R_3= H
6i: R'=CH_3CO, R_1= H, R_2=H, R_3= NH_2
6j: R'=CH_3CO, R_1=OH, R_2=H, R_3= H
6k: R'=CH_3CO, R_1= H, R_2=OH, R_3= H
6l: R'=CH_3CO, R_1= H, R_2=H, R_3= OH
6m: R'=$NHCOCH_3$, R_1=NH_2, R_2=H, R_3= H
6n: R'=$NHCOCH_3$, R_1= H, R_2=NH_2, R_3= H
6o: R'=$NHCOCH_3$, R_1= H, R_2=H, R_3= NH_2
6p: R'=$NHCOCH_3$, R_1=OH, R_2=H, R_3= H
6q: R'=$NHCOCH_3$, R_1= H, R_2=OH, R_3= H
6r: R'=$NHCOCH_3$, R_1= H, R_2=H, R_3= OH
6s: R'=NO_2, R_1=OCH_3, R_2=OCH_3, R_3= H
6t: R'=CH_3CO, R_1=OCH_3, R_2=OCH_3, R_3= H
6u: R'=$NHCOCH_3$, R_1=OCH_3, R_2=OCH_3, R_3= H

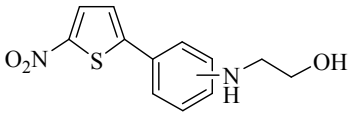

7a (ortho position)
7b (meta position)
7c (para position)

Figure 6. A: Binding pose of compound **6a** into the ATP-binding site of WalK. **B:** Evaluation of compound **6a** docked into ATP-Binding site using PLANTS with DSX. Blue spheres represent favorable interactions whereas red spheres represents bad interactions. Blue lines represent favorable distances whereas red lines represent bad distances.

A

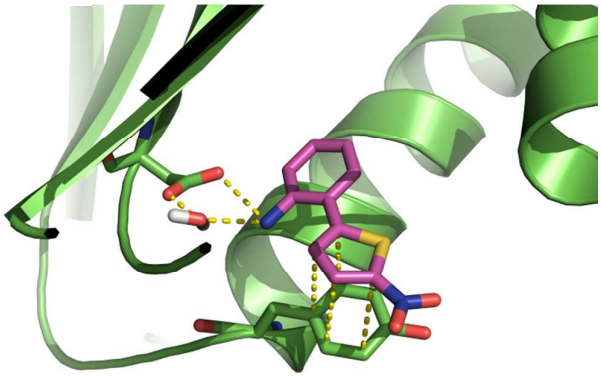

B

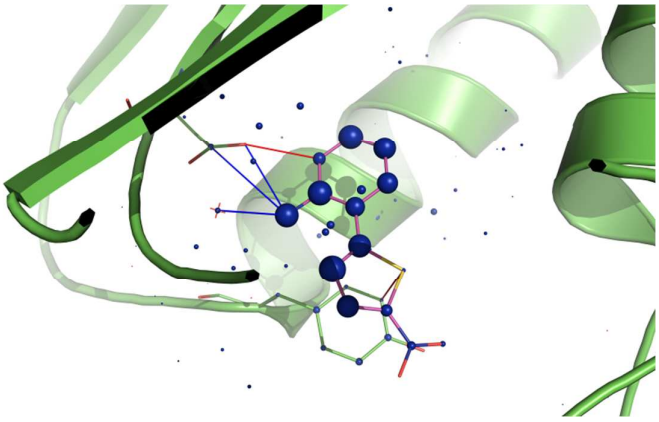

Figure 7. A screen with cytoplasmic WalK fragments identifies eight compounds with kinase inhibitory activity.

Two *Bacillus subtilis* cytoplasmic histidine kinases constructs, $WalK^{272-612}$ and $WalK^{204-612}$, were subjected to autophosphorylation in the presence of 1 mM**γ**-^{32}P-labeled ATP and in the presence or absence (control) of 1 mM of putative kinase inhibitors. Autophosphorylation of WalK kinase was terminated after 3 minutes by addition of SDS-sample buffer and the reactions were subjected to SDS-PAGE followed by phosphor-imaging. Bands on the gel indicate the extent of the autophosphorylation reaction. Compounds, whose presence caused visual reduction in autophosphorylation activity are indicated by an arrow and were selected for further analysis**. (A)** Compounds used were **6g**, **6h**, **6b**, **7a**, **6c**, **6a**, **6j**, and **6k**; top panel $WalK^{204-612}$; bottom panel $WalK^{272-612}$. **(B)** Compounds used were **6t**, **6s**, **6d**, **6e**, **6f**, **6m**, **6o**, and **6u**; top panel $WalK^{204-612}$; bottom Panel $WalK^{272-612}$. **(C)** Compounds used were **7c**, **6i**, **6l**, **6n**, **7b**, **6p**, **6q**, and **6r**; top panel $WalK^{204-612}$; bottom panel $WalK^{272-612}$.

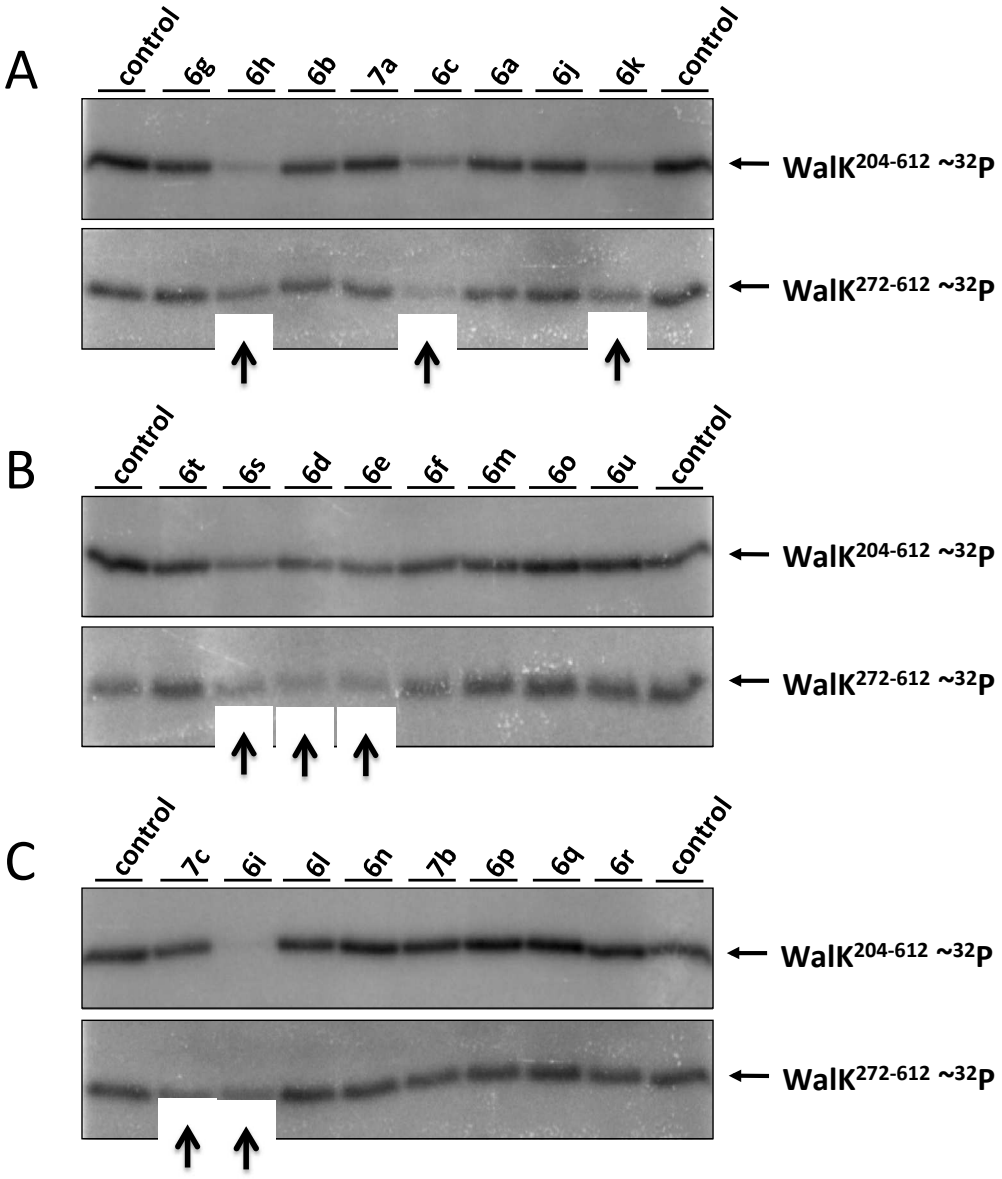
A
control
6g
6h
6b
7a
6c
6a
6j
6k
control
WalK204-612 ~32P
WalK272-612 ~32P
B
control
6t
6s
6d
6e
6f
6m
6o
6u
control
WalK204-612 ~32P
WalK272-612 ~32P
C
control
7c
6i
6l
6n
7b
6p
6q
6r
control
WalK204-612 ~32P
WalK272-612 ~32P

Figure 8. Compound **6e** inhibits autophosphorylation of histidine kinases PhoR, ResE and WalK but not serine/threonine kinase IreK or DNA-gyrase.

Autophosphorylation of kinases and DNA gyrase-catalyzed supercoiling were performed as described in materials and methods. In contrast to Figure 1, protein concentrations, ATP concentrations and time points were adjusted for IC_{50} determination. **(A)** Autophosphorylation activity of cytoplasmic constructs of PhoR (top panel), ResE (middle panel) and WalK (bottom panel) in the presence of increasing amounts of compound **6e** (0; 6.25; 12.5; 25; 50; 100; 200; 400; 800 μM). The autophosphorylation activity was monitored after 60, 8 and 40 min respectively. These time points were chosen imperially to reflect a linear rate of autophosphorylation for each kinase. **(B)** The serine/threonine kinase IreK from *E. faecalis* was subjected to autophosphorylation in analogy to the assays performed for histidine kinases with increasing amounts of compound **6e** (0; 6.25; 12.5; 25; 50; 100; 200; 400; and 800 μM). The autophosphorylation activity was monitored after 15 min. **(C)** *E. coli* DNA gyrase-catalyzed supercoiling in the presence and absence of indicated concentrations of compound **6e** was monitored. Ciprofloxacin (200 nM) was used as a positive control for gyrase inhibition. Each reaction contained 1U gyrase and 75ng gyrase substrate according to manufacturer recommendation.

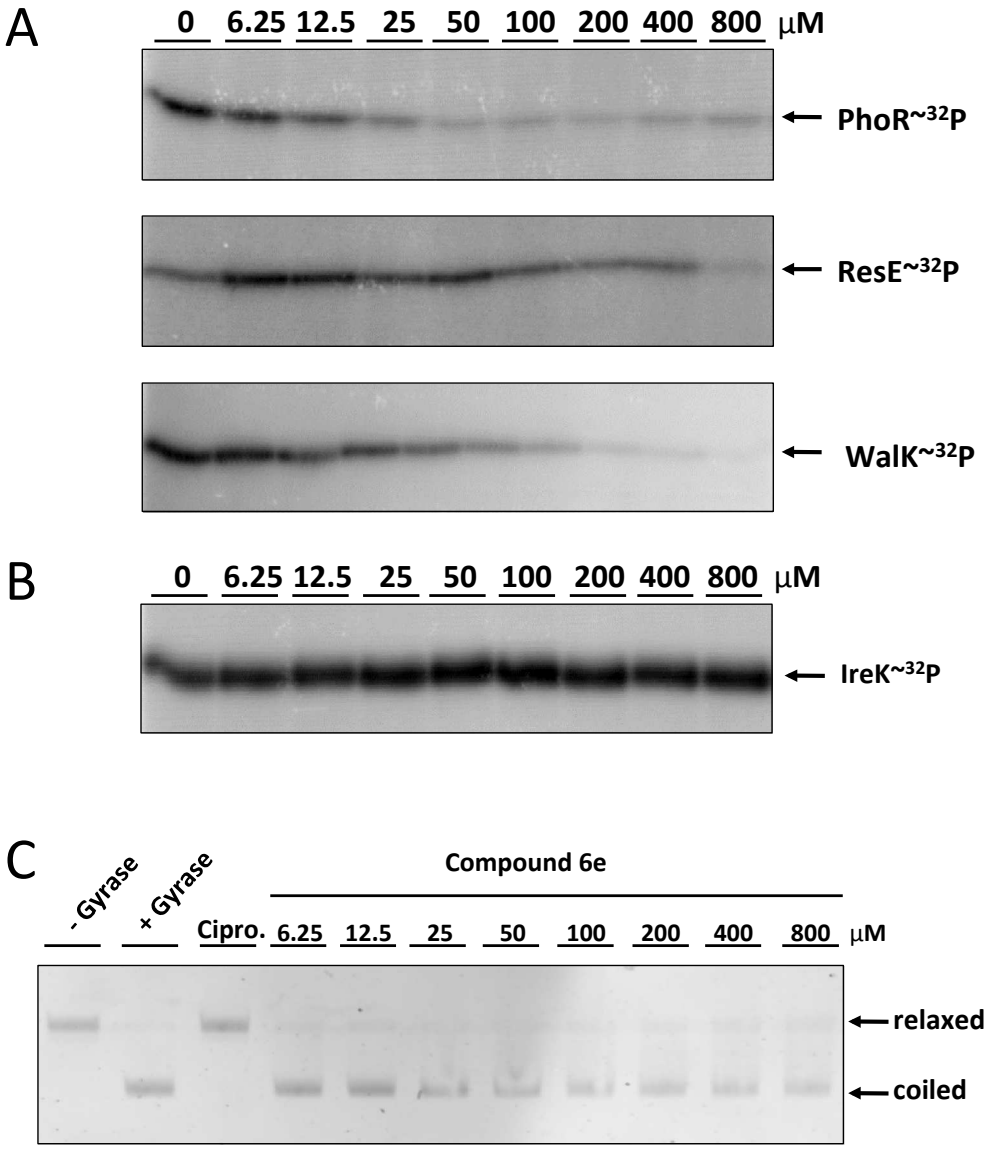
A
0 6.25 12.5 25 50 100 200 400 800 μM
PhoR~32P
ResE~32P
WalK~32P
B
0 6.25 12.5 25 50 100 200 400 800 μM
IreK~32P
C
- Gyrase
+ Gyrase
Compound 6e
Cipro.
6.25 12.5 25 50 100 200 400 800 μM
relaxed
coiled

Figure 9. The histidine kinase inhibitors **6d** and **6e** exhibit antimicrobial activity (A, B).
The Kirby-Bauer disk diffusion susceptibility assay was used to determine the antimicrobial activity of the selected compounds (see material and methods). **(A)** Antimicrobial activity screen of the eight selected compounds against methicillin resistant *S. aureus* (MRSA). A disk containing 30µg vancomycin was used as control (c). 100µg of compounds **6h** (1), **6c** (2), **6k** (3), **6s** (4), **6d** (5), **6e** (6), **7c** (7) and **6i** (8) was applied to each disk. **(B)** Dose-dependent antimicrobial activities of the compounds **6d** and **6e** against MRSA. 30µg vancomycin was used as control (c). Decreasing amounts of **6d** (left) and **6e** (right). [1 and 7 = 500 µg; 2 and 8 = 100 µg; 3 and 9 = 20 µg; 4 and 10 = 4 µg; 5 and 11 = 0.8 µg ; 6 and 12 = 0.16 µg] **(C)** Effect of compounds **6d** and **6e** on exponentially growing *B. subtilis* cultures was monitored. To determine whether compounds **6d** and **6e** exhibit bactericidal or bacteriostatic activity *B. subtilis* JH642 was grown in LB medium at 37 °C. Vancomycin (Va) and chloramphenicol (Cm) served as controls. Optical density (OD) at a wavelength of 600 nm was routinely measured. At an OD_{600} of 0.5-0.6 (indicated by an arrow) 50µg compounds **6d** (squares), **6e** (triangles facing up), chloramphenicol (triangles facing down) or vancomycin (diamonds) was added. *B. subtilis* JH642 was also grown without additives (circles).

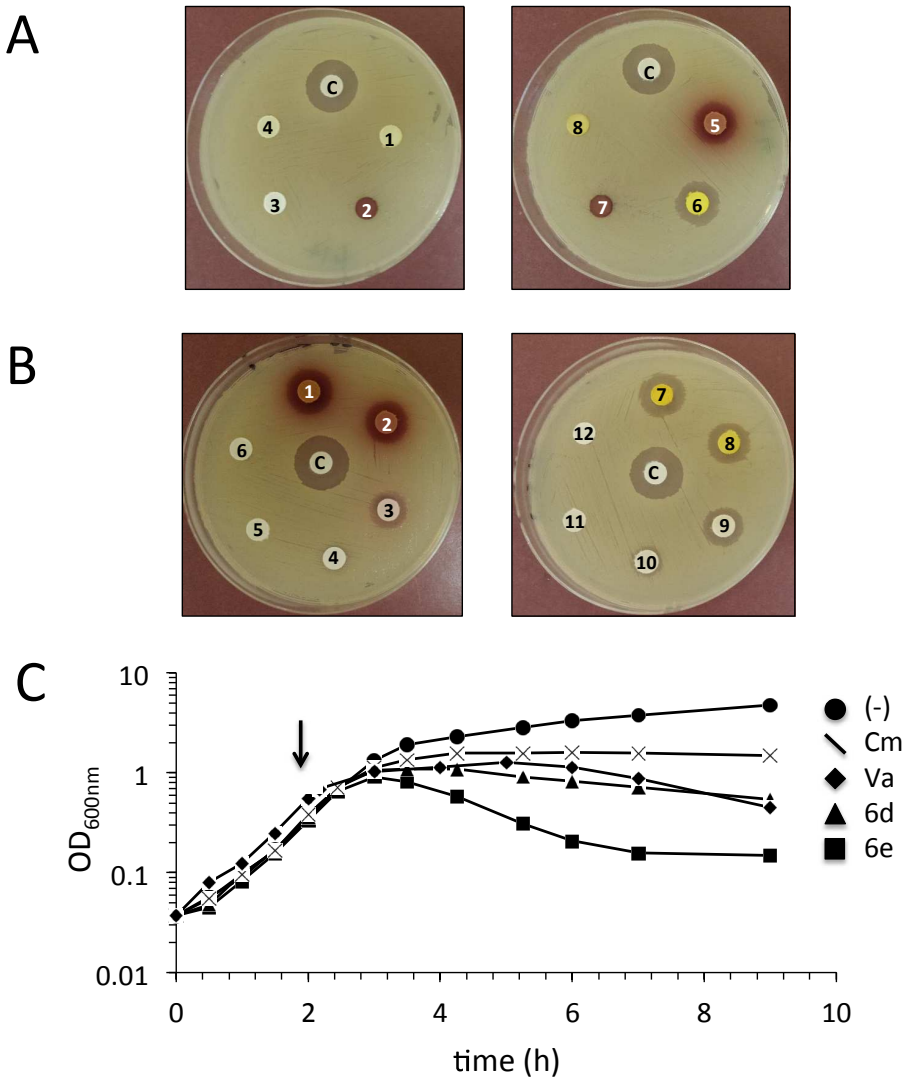
A
C
4
1
3
2
C
8
5
7
6
B
1
2
6
C
3
5
4
7
12
8
C
11
9
10
C
10
1
0.1
0.01
OD600nm
0
2
4
6
8
10
time (h)
(-)
Cm
Va
6d
6e

Scheme 1. Synthesis of Thiophene derivatives **6a-u**[a]

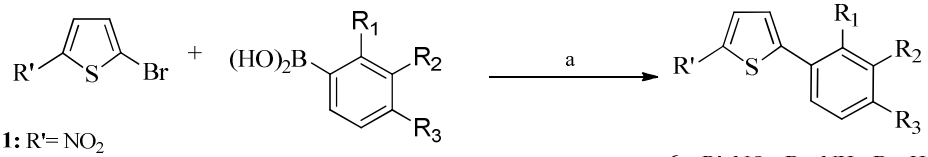

1: R'= NO_2
2: R'= CH_3CO
3: R'= $NHCOCH_3$

5a: R_1=NH_2HCl, R_2=H, R_3=H
5b: R_1=H, R_2=NH_2HCl, R_3=H
5c: R_1=H, R_2=H, R_3=NH_2HCl
5d: R_1=OH, R_2=H, R_3= H
5e: R_1= H, R_2=OH, R_3= H
5f: R_1= H, R_2=H, R_3= OH
5g: R_1=OCH_3, R_2=OCH_3, R_3= H

6a: R'=NO_2, R_1=NH_2, R_2=H, R_3= H
6b: R'=NO_2, R_1= H, R_2=NH_2, R_3= H
6c: R'=NO_2, R_1= H, R_2=H, R_3= NH_2
6d: R'=NO_2, R_1=OH, R_2=H, R_3= H
6e: R'=NO_2, R_1= H, R_2=OH, R_3= H
6f: R'=NO_2, R_1= H, R_2=H, R_3= OH
6g: R'=CH_3CO, R_1=NH_2, R_2=H, R_3= H
6h: R'=CH_3CO, R_1= H, R_2=NH_2, R_3= H
6i: R'=CH_3CO, R_1= H, R_2=H, R_3= NH_2
6j: R'=CH_3CO, R_1=OH, R_2=H, R_3= H
6k: R'=CH_3CO, R_1= H, R_2=OH, R_3= H
6l: R'=CH_3CO, R_1= H, R_2=H, R_3= OH
6m: R'=$NHCOCH_3$, R_1=NH_2, R_2=H, R_3= H
6n: R'=$NHCOCH_3$, R_1= H, R_2=NH_2, R_3= H
6o: R'=$NHCOCH_3$, R_1= H, R_2=H, R_3= NH_2
6p: R'=$NHCOCH_3$, R_1=OH, R_2=H, R_3= H
6q: R'=$NHCOCH_3$, R_1= H, R_2=OH, R_3= H
6r: R'=$NHCOCH_3$, R_1= H, R_2=H, R_3= OH
6s: R'=NO_2, R_1=OCH_3, R_2=OCH_3, R_3= H
6t: R'=CH_3CO, R_1=OCH_3, R_2=OCH_3, R_3= H
6u: R'=$NHCOCH_3$, R_1=OCH_3, R_2=OCH_3, R_3= H

[a]Reagents and conditions: (a) $Pd(PPh_3)_4$ or $PdCl_2(PPh_3)_2$, Na_2CO_3 or K_2CO_3 or Cs_2CO_3, Toluene/EtOH or 1,4-dioxane/H_2O or DMF/H_2O or DMF, 70-90°C.

Scheme 2. Synthesis of acetamide **3**[a]

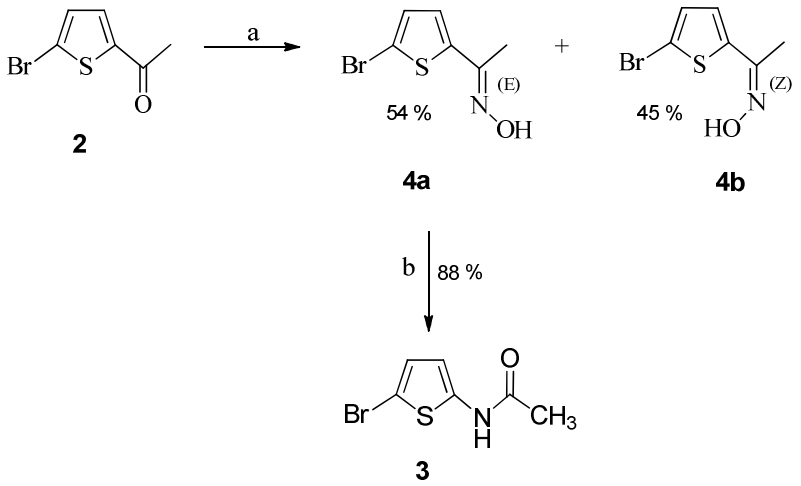

[a]Reagents and conditions: (a) NH_2OH-HCl, CH_3COONa-$3H_2O$; (b) TsCl, NaOH.

Scheme 3. Synthesis of Thiophene derivatives **7a-c**[a]

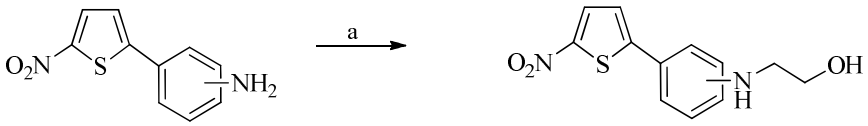

6a (ortho position)
6b (meta position)
6c (para position)

7a (ortho position)
7b (meta position)
7c (para position)

[a]Reagents and conditions: (a) $I(CH_2)_2OH$, 90°C, N_2.

Scheme 4. Synthesis of amine hydrochloride salts **8a-i**[a]

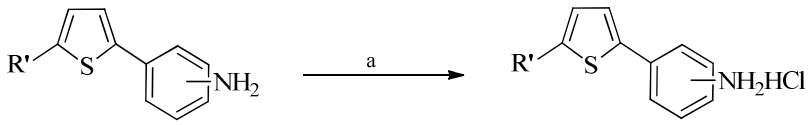

6a: R'=NO_2, R_1=NH_2, R_2=H, R_3= H
6b: R'=NO_2, R_1= H, R_2=NH_2, R_3= H
6c: R'=NO_2, R_1= H, R_2=H, R_3= NH_2
6g: R'=CH_3CO, R_1=NH_2, R_2=H, R_3= H
6h: R'=CH_3CO, R_1= H, R_2=NH_2, R_3= H
6i: R'=CH_3CO, R_1= H, R_2=H, R_3= NH_2
6m: R'=$NHCOCH_3$, R_1=NH_2, R_2=H, R_3= H
6n: R'=$NHCOCH_3$, R_1= H, R_2=NH_2, R_3= H
6o: R'=$NHCOCH_3$, R_1= H, R_2=H, R_3= NH_2

8a: R'=NO_2, R_1=NH_2HCl, R_2=H, R_3= H, 37%
8b: R'=NO_2, R_1= H, R_2=NH_2HCl, R_3= H, 89%
8c: R'=NO_2, R_1= H, R_2=H, R_3= NH_2HCl, 59%
8d: R'=CH_3CO, R_1=NH_2HCl, R_2=H, R_3= H, 96%
8e: R'=CH_3CO, R_1= H, R_2=NH_2HCl, R_3= H, 35%
8f: R'=CH_3CO, R_1= H, R_2=H, R_3= NH_2HCl, 39%
8g: R'=$NHCOCH_3$, R_1=NH_2HCl, R_2=H, R_3= H, 49%
8h: R'=$NHCOCH_3$, R_1= H, R_2=NH_2HCl, R_3= H, 46%
8i: R'=$NHCOCH_3$, R_1= H, R_2=H, R_3= NH_2HCl, 51%

[a]Reagents and conditions: (a) HCl 12M, THF, 0°C or HCl generated in situ (Addition of concd H_2SO_4 on NaCl)

Table1. DSX score of docked compounds.

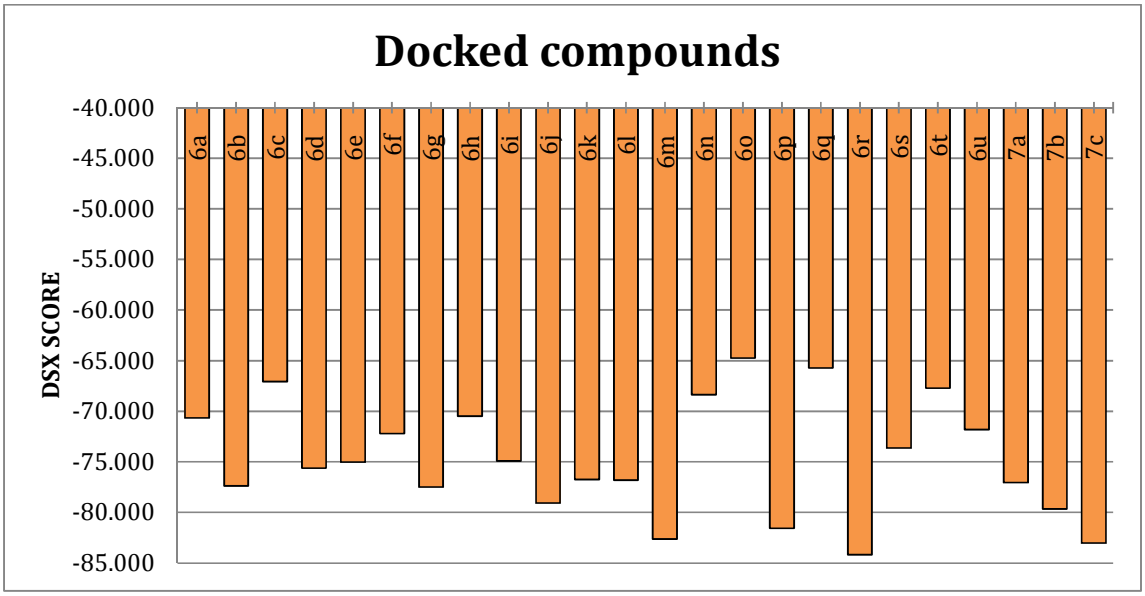

Table 2. Chemical structure, chemical data and purity of synthesized compounds.

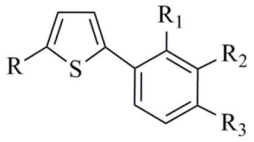

Compound	R	R1	R2	R3	Yield[a] (%)	M.P (°C)	Purity[b] (%)
6a	NO_2	NH_2	H	H	30	101-103	100
6b	NO_2	H	NH_2	H	60	127-129	97
6c	NO_2	H	H	NH_2	66	208-210	96
6d	NO_2	OH	H	H	42	176-178	98
6e	NO_2	H	OH	H	42	182-184	98
6f	NO_2	H	H	OH	51	235-237	99
6g	Ac	NH_2	H	H	56	127-129	100
6h	Ac	H	NH_2	H	77	155-157	97
6i	Ac	H	H	NH_2	41	174-176	97
6j	Ac	OH	H	H	65	211-213	99
6k	Ac	H	OH	H	50	172-174	100
6l	Ac	H	H	OH	40	211-213	96
6m	NHAc	NH_2	H	H	52	157-159	99
6n	NHAc	H	NH_2	H	23	220-222	99
6o	NHAc	H	H	NH_2	66	169-171	100
6p	NHAc	OH	H	H	35	205-207	100
6q	NHAc	H	OH	H	73	144-146	100
6r	NHAc	H	H	OH	67	207-209	100
6s	NO_2	OCH_3	OCH_3	H	54	126-128	100
6t	Ac	OCH_3	OCH_3	H	17	122-124	100
6u	NHAc	OCH_3	OCH_3	H	45	124-126	100
7a	NO_2	NH-$(CH_2)_2$-OH	H	H	37	91-93	97
7b	NO_2	H	NH-$(CH_2)_2$-OH	H	42	103-105	98
7c	NO_2	H	H	NH-$(CH_2)_2$-OH	31	164-166	99

[a]Yields obtained after purification (flash chromatography, precipitation with pentane/EtOAc or recrystallization) from Suzuki coupling for compounds **6a-6u** (Scheme 1) and from nucleophilic Substitution for compounds **7a-c** (Scheme 2) [b]HPLC purity.

Table 3. Conditions of Suzuki coupling to obtain Thiophene derivatives **6a-u** and **7a-c**.

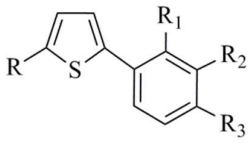

Entry	Compound	Pd catalyst	Base	Solvent(s)	Time (hours)	Temperature (°C)
1	**6a**	$Pd(PPh_3)_4$	Na_2CO_3 (2M)	Toluene/EtOH	16	90
2	**6b**	$Pd(PPh_3)_4$	Na_2CO_3 (2M)	Toluene/EtOH	16	90
3	**6c**	$Pd(PPh_3)_4$	Na_2CO_3 (2M)	Toluene/EtOH	16	90
4	**6d**	$Pd(PPh_3)_4$	K_2CO_3	1,4-dioxane/ H_2O	6	80
5	**6e**	$Pd(PPh_3)_4$	K_2CO_3	1,4-dioxane/ H_2O	6	80
6	**6f**	$Pd(PPh_3)_4$	K_2CO_3	1,4-dioxane/ H_2O	6	80
7	**6g**	$Pd(PPh_3)_4$	Na_2CO_3 (2M)	Toluene/EtOH	16	90
8	**6h**	$Pd(PPh_3)_4$	Na_2CO_3 (2M)	Toluene/EtOH	16	90
9	**6i**	$Pd(PPh_3)_4$	Na_2CO_3 (2M)	Toluene/EtOH	16	90
10	**6j**	$Pd(PPh_3)_4$	K_2CO_3	1,4-dioxane/H_2O	6	80
11	**6k**	$Pd(PPh_3)_4$	K_2CO_3	1,4-dioxane/H_2O	6	80
12	**6l**	$Pd(PPh_3)_4$	K_2CO_3	1,4-dioxane/H_2O	6	80
13	**6m**	$PdCl_2(PPh_3)_2$	K_2CO_3 (2M)	DMF	1	70
14	**6n**	$PdCl_2(PPh_3)_2$	K_2CO_3 (2M)	DMF	1	70
15	**6o**	$PdCl_2(PPh_3)_2$	K_2CO_3 (2M)	DMF	1	70
16	**6p**	$PdCl_2(PPh_3)_2$	Cs_2CO_3	DMF/H_2O	3	80
17	**6q**	$PdCl_2(PPh_3)_2$	Cs_2CO_3	DMF/H_2O	3	80
18	**6r**	$PdCl_2(PPh_3)_2$	Cs_2CO_3	DMF/H_2O	3	80
19	**6s**	$Pd(PPh_3)_4$	K_2CO_3	1,4-dioxane/ H_2O	6	80
20	**6t**	$Pd(PPh_3)_4$	K_2CO_3	1,4-dioxane/ H_2O	15	80
21	**6u**	$PdCl_2(PPh_3)_2$	K_2CO_3	DMF/H_2O	3	80

Table 4. IC_{50} values against histidine kinases PhoR, ResE and WalK, Ser/Thr kinase IreK and DNA-gyrase for selected compounds.

Compound	PhoR	ResE	WalK	IreK	DNA-gyrase
6h	46.18 μM	20.3 μM	145.6 μM	>800 μM	>800 μM
6c	21.37 μM	52.28 μM	181.1 μM	>800 μM	>400 μM
6k	44.02 μM	32.85 μM	78.37 μM	>800 μM	>400 μM
6s	1.63 μM	102.3 μM	134.4 μM	>800 μM	>800 μM
6d	122.6 μM	124.3 μM	196.9 μM	>800 μM	≥400 μM
6e	13.11 μM	89.36 μM	52.81 μM	>800 μM	>800 μM
7c	11.39 μM	243.9 μM	80.11 μM	>800 μM	>400 μM
6i	33.39 μM	40.38 μM	121.3 μM	>800 μM	>800 μM

Table 5. Antibacterial activity of compounds **6d** and **6e** against reference Gram-positive and Gram-negative bacteria. Minimal inhibitory concentration (MIC) and minimal bactericidal concentration (MBC) are in μg/ml.

	Compound 6d		Compound 6e	
Bacterial strain	**MIC**	**MBC**	**MIC**	**MBC**
B. subtilis	7	10	7	16
S. aureus	16	32	32	>32
B.anthracis	7	16	7	>32
S. pyogenes	10	32	16	32
S. agalactiae	16	>32	32	>32
L. monocytogenes	10	>64	32	>64
E. faecalis	32	>64	>64	>64
S. enterica	32	32	32	32
E. coli	32	32	32	32

Table 6. Antibiotic susceptibility of four *Escherichia coli* isolates and three *Staphylococcus aureus* isolates with and without histidine kinase inhibitor **6d**.

Bacterial Strains	Resistance Mechanism	MICs[a] (µg/ml) [with 6d][b] AMX (≤8, >8)[c]	CTX (≤1, >2)	OFX (≤0.5, >1)	CLX (≤2, >2)	PNG (≤0.125, >0.125)
E. coli[f]						
ATCC25922	none	4	0.125	0.06	-	-
G28	BL	>16 [0.03]	>16 [0.03]	-	-	-
ARS108	BLSE	>16 [0.03]	>16 [0.03]	-	-	-
G02	R FQ	-	-	>8 [<0.015]	-	-
S. aureus[g]						
ATCC29213	none	-	-	-	1	0.5
C1P15	Penicillinase	-	-	-	1	>8 [<0.015]
C1BP13	MRSA	-	-	-	>8 [<0.015]	>8 [<0.015]
		MBCs[d] (µg/ml) [with 6d][e]				
E. coli						
ATCC25922	none	-	-	-	-	-
G28	BL	>16 [8]	1	-	-	-
ARS108	BLSE	>16 [>16]	>8 [>8]	-	-	-
G02	R FQ	-	-	>8 [>8]	-	-
S. aureus						
ATCC29213	none	-	-	-	1	0.5
C1P15	Penicillinase	-	-	-	1	>8 [2]
C1BP13	MRSA	-	-	-	>8 [>8]	>8 [4]

[a] MICs, Minimum Inhibitory Concentrations; AMX, amoxicillin; CTX, cefotaxime; OFX, ofloxacin;. CLX, cloxacillin ; PNG, penicillin G.
[b] The MICs values obtained in the presence of TCS inhibitors (**6d** at 50µg/mL) are shown in brackets.
[c] The breakpoints according to the European Committee on Antimicrobial Susceptibility Testing (EUCAST) are given in parentheses.
[d] MBCs, Minimum Bactericidal Concentration.
[e] The MBC values obtained in the presence of TCS inhibitors (**6d** at 50µg/mL) are shown in brackets.
[f] Three clinical isolates of *E. coli* have been tested: G28: *E. coli* with beta lactamase; ARS 108: *E. coli* with Extended Spectrum Beta Lactamase (ESBL); G02: ofloxacin-resistant *E. coli*; ATCC25922: quality control strain
[g] Two clinical isolates of *S. aureus* have been tested: C1P15: *S. aureus* with penicillinase;C1BP13: Meticillin Resistant *S. aureus* (MRSA); ATCC29213: quality control strains

Table of contents graphic

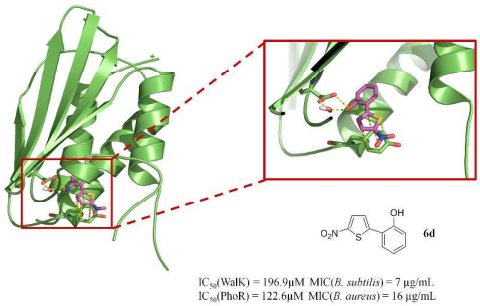
OH
O_2N
S
6d
IC_{50}(WalK) = 196.9μM MIC(*B. subtilis*) = 7 μg/mL
IC_{50}(PhoR) = 122.6μM MIC(*B. aureus*) = 16 μg/mL